Chapter 8

LONGITUDINAL COUPLED-BUNCH INSTABILITIES

When the wake does not decay within the bunch spacing, bunches talk to each other. Assuming M bunches of equal intensity equally spaced in the ring, there are $\mu = 0,\ 1,\ \cdots,\ M-1$ modes of oscillations in which the center-of-mass of a bunch *leads*[*] its predecessor by the phase $2\pi\mu/M$. In addition, an individual bunch in the μ-th coupled-bunch mode can oscillate in the synchrotron phase space about its center-of-mass in such a away that there are $m = 1,\ 2,\ \cdots$ azimuthal nodes in the perturbed longitudinal phase-space distribution. Of course, there will be in addition radial modes of oscillation in the perturbed distribution. The long-range wake can drive the coupled bunches to instability.

8.1 SACHERER INTEGRAL EQUATION

Because the beam particles execute synchrotron oscillations, it is more convenient to use circular coordinates r, ϕ in the longitudinal phase space instead. We define

$$\begin{cases} x \ = r\cos\phi = \tau \ , \\ p_x = r\sin\phi = \dfrac{\eta}{\omega_s\beta^2}\dfrac{\Delta E}{E_0} \ , \end{cases} \tag{8.1}$$

[*]We can also formulate the problem by having the bunch *lag* its predecessor by the phase $2\pi\mu'/M$ in the μ'-th coupling mode. Then mode μ' will be exactly the same as mode $M-\mu$ discussed in the text.

so that the equations of motion become

$$\begin{cases} \dfrac{dx}{ds} = -\dfrac{\omega_s}{v} p_x \ , \\ \dfrac{dp_x}{ds} = \dfrac{\omega_s}{v} x + \dfrac{\eta}{E_0 \omega_s \beta^2} \langle F_0^{\parallel}(\tau; s) \rangle \ . \end{cases} \tag{8.2}$$

The phase-space distribution ψ of a bunch can be separated into the unperturbed or stationary part ψ_0 and the perturbed part ψ_1:

$$\psi(\tau, \Delta E; s) = \psi_0(\tau, \Delta E) + \psi_1(\tau, \Delta E; s) \ . \tag{8.3}$$

The linearized Vlasov equation becomes

$$\frac{\partial \psi_1}{\partial s} - \frac{\omega_s}{v} p_x \frac{\partial \psi_1}{\partial x} + \frac{\omega_s}{v} x \frac{\partial \psi_1}{\partial p_x} + \frac{\partial \psi_0}{\partial p_x} \frac{\eta}{E_0 \omega_s \beta^2} \langle F_0^{\parallel}(\tau; s) \rangle = 0 \ . \tag{8.4}$$

Changing to the circular coordinates, the equation simplifies to

$$\frac{\partial \psi_1}{\partial s} + \frac{\omega_s}{v} \frac{\partial \psi_1}{\partial \phi} + \frac{\eta}{E_0 \omega_s \beta^2} \frac{d\psi_0}{dr} \sin\phi \langle F_0^{\parallel}(\tau; s) \rangle = 0 \ . \tag{8.5}$$

The perturbed distribution can be expanded azimuthally,

$$\psi_1(r, \phi; s) = \sum_m \alpha_m R_m(r) e^{im\phi - i\Omega s/v} \ , \tag{8.6}$$

where $R_m(r)$ are functions corresponding to the m-th azimuthal, α_m are the expansion coefficients, and $\Omega/(2\pi)$ is the collective frequency to be determined. The Vlasov equation becomes

$$(\Omega - m\omega_s) \alpha_m R_m(r) e^{-i\Omega s/v} = -\frac{iv\eta}{E_0 \omega_s \beta^2} \frac{d\psi_0}{dr} \int_{-\pi}^{\pi} \frac{d\phi}{2\pi} e^{-im\phi} \sin\phi \, \langle F_0^{\parallel}(\tau; s) \rangle \ . \tag{8.7}$$

Now consider the wake force acting on a beam particle at location s with time advance τ relative to the synchronous particle due to all preceding particles passing through s at an earlier time. This force can be expressed as

$$\langle F_0^{\parallel}(\tau; s) \rangle = -\frac{e^2}{C} \sum_{k=-\infty}^{\infty} \int_{-\infty}^{\infty} d\tau' \rho_1[\tau', s - kC - v(\tau' - \tau)] W_0'[kC + v(\tau' - \tau)] \ , \tag{8.8}$$

where only the perturbed density ρ_1, which is the projection of ψ_1 onto the τ axis, is included, because the unperturbed part should have been considered in the zeroth order

of the Vlasov equation during the discussion of potential-well distortion. The summation over k takes care of the contribution of the wake left by the charge distribution in previous turns. The lower limit of the summation and the lower limit of the integral have been extended to $-\infty$ because of the causality property of the wake function. Now there are M bunches and the synchronous particle in the ℓ-th bunch is at location s_ℓ. If the witness particle is in the n-th bunch,

$$\langle F^{\parallel}_{0n}(\tau;s)\rangle = -\frac{e^2}{C}\sum_{k=-\infty}^{\infty}\sum_{\ell=0}^{M-1}\int_{-\infty}^{\infty} d\tau' \rho_\ell[\tau';s-kC-(s_\ell-s_n)-v(\tau'-\tau)]W'_0[kC+(s_\ell-s_n)+v(\tau'-\tau)]\,. \tag{8.9}$$

We assume the bunches are identical and equally spaced. For the μ-th coupled mode, we substitute in the above expression the perturbed density of the n-th bunch $\rho_{1n}(\tau)e^{-i\Omega s/v}$ including the phase lead,

$$\rho_\ell(\tau;s) = \rho_{1n}(\tau)e^{i2\pi\mu(\ell-n)/M}e^{-i\Omega s/v}\ . \tag{8.10}$$

Now go to the frequency domain using the Fourier transforms

$$W'_0(v\tau) = \frac{1}{2\pi}\int_{-\infty}^{\infty} d\omega\, Z^{\parallel}_0(\omega)e^{-i\omega\tau}\ , \tag{8.11}$$

$$\rho_{1n}(\tau;s) = \int_{-\infty}^{\infty} d\omega\, \tilde\rho_{1n}(\omega)e^{i\omega\tau}\ . \tag{8.12}$$

In Eq. (8.9) above, we shall neglect[†] the time delay $\tau'-\tau$ because this will only amount to a phase delay $\Omega(\tau'-\tau)$ where $\Omega \approx m\omega_s$, which is very much less than the phase change $\omega_r(\tau'-\tau)$ during the bunch passage, where $\omega_r/(2\pi)$ is the frequency of the driving resonant impedance. Substituting Eqs. (8.11) and (8.12) into Eq. (8.9) and integrating over τ' and one of the ω's, the wake force for the μ-th coupled-bunch mode becomes

$$\langle F^{\parallel}_{0n\mu}(\tau;s)\rangle = -\frac{e^2}{C}\sum_{k=-\infty}^{\infty}\sum_{\ell=0}^{M-1} e^{i2\pi\mu(\ell-n)/M}e^{i\Omega(-s+kC+s_\ell-s_n)/v}\times \\ \times\int_{-\infty}^{\infty} d\omega\tilde\rho_{1n}(\omega)Z^{\parallel}_0(\omega)e^{-i\omega(kC+s_\ell-s_n)/v}e^{i\omega\tau}\,. \tag{8.13}$$

[†]Without this approximation, only $Z^{\parallel}_0$ will have the argument ω_q in Eq. (8.16) below. The argument of $\tilde\rho$ and the factor in front of τ in the exponent will be replaced by $\omega_q-\Omega$.

Now the summation over k can be performed giving

$$\langle F^{\parallel}_{0n\mu}(\tau;s)\rangle = -\frac{e^2}{C}\sum_{p=-\infty}^{\infty}\sum_{\ell=0}^{M-1} e^{i2\pi\mu(\ell-n)/M} e^{-i\Omega s/v + i\omega_p\tau}\omega_0\tilde{\rho}_{1n}(\omega_p)Z_0^{\parallel}(\omega_p)e^{-ip\omega_0(s_\ell - s_n)/v}\,, \tag{8.14}$$

where $\omega_p = p\omega_0 + \Omega$. We next make use of the fact that the unperturbed bunches are equally spaced, or

$$s_\ell - s_n = \frac{\ell - n}{M}\,C\ . \tag{8.15}$$

Then the summation over ℓ can be performed. The sum vanishes unless $(p-\mu)/M = q$, where q is an integer. The final result is

$$\langle F^{\parallel}_{0n\mu}(\tau;s)\rangle = -\frac{e^2 M\omega_0}{C}\,e^{-i\Omega s/v}\sum_{q=-\infty}^{\infty}\tilde{\rho}_{1n}(\omega_q)Z_0^{\parallel}(\omega_q)e^{i\omega_q\tau}\ , \tag{8.16}$$

where $\omega_q = (qM+\mu)\omega_0 + \Omega$.

Since the left side of the Vlasov equation is expressed in terms of the radial function $R_m(r)$, we want to do the same for the wake force. First, rewrite the perturbed density in the time domain,

$$\langle F^{\parallel}_{0n\mu}(\tau;s)\rangle = -\frac{e^2 M\omega_0}{C}\,e^{-i\Omega s/v}\sum_{q=-\infty}^{\infty}Z_0^{\parallel}(\omega_q)\int\frac{d\tau'}{2\pi}\,\rho_{1n}(\tau')e^{i\omega_q(\tau-\tau')}\ . \tag{8.17}$$

Since $\rho_1(\tau')$ is the projection of the perturbed distribution onto the τ' axis, we must have

$$\rho_{1n}(\tau')d\tau' = \int\psi_{1n}(\tau',\Delta E')d\tau' d\Delta E' \tag{8.18}$$

$$= \frac{E_0\omega_s\beta^2}{\eta}\int\psi_{1n}(r',\phi')r'dr'd\phi' \tag{8.19}$$

$$= \frac{E_0\omega_s\beta^2}{\eta}\sum_{m'}\alpha_{m'}\int R_{m'}(r')e^{im'\phi'}r'dr'd\phi'\ . \tag{8.20}$$

The wake force then takes the form

$$\langle F^{\parallel}_{0n}(\tau;s)\rangle = -\frac{e^2\omega_0 M}{2\pi C}\frac{E_0\omega_s\beta^2}{\eta}\,e^{-i\Omega s/v}\sum_{q=-\infty}^{\infty}\sum_{m'}Z_0^{\parallel}(\omega_q)\int r'dr'd\phi'\alpha_{m'}R_{m'}(r')e^{im'\phi'}e^{i\omega_q(\tau-\tau')}\,, \tag{8.21}$$

This wake force is next substituted into the Vlasov equation (8.7). The integrations over ϕ and ϕ' are performed in terms of Bessel function of order m using its integral definition

$$i^m J_m(z) = \frac{1}{2\pi}\int_{-\pi}^{\pi} d\phi\, e^{\pm im\phi + iz\cos\phi} \ , \tag{8.22}$$

the recurrence relation

$$J_{m-1}(z) + J_{m+1}(z) = \frac{2m}{z} J_m(z) \ , \tag{8.23}$$

and the fact that

$$J_m(-z) = (-1)^m J_m(z) \ . \tag{8.24}$$

The result is the Sacherer integral equation for longitudinal instability for the m-th azimuthal μ-th coupled-bunch mode,

$$(\Omega - m\omega_s)\alpha_m R_m(r) = -\frac{i2\pi e^2 MN\eta}{\beta^2 E_0 T_0^2 \omega_s}\frac{m}{r}\frac{dg_0}{dr}\sum_{m'} i^{\,m-m'}\alpha_{m'}\int r'dr' R_{m'}(r')\sum_q \frac{Z_0^{\parallel}(\omega_q)}{\omega_q} J_{m'}(\omega_q r') J_m(\omega_q r) \ , \tag{8.25}$$

where transformation of the unperturbed longitudinal distribution

$$\psi_0(r)d\tau d\Delta E = \frac{\omega_s\beta^2 E_0}{\eta}\,\psi_0 dx dp_x = N g_0(r) r dr d\phi \tag{8.26}$$

has been made so that g_0 is normalized to unity when integrated over $rdrd\phi$.

This is an eigen-function-eigen-value problem, the α_m's being the eigen-functions and Ω the corresponding eigen-value. The solution is nontrivial. However, with some approximations, interesting results can be deduced. When the perturbation is not too strong so that the shift in frequency is much less than the synchrotron frequency, there will not be coupling between different azimuthals. The integral equation simplifies to

$$(\Omega - m\omega_s)R_m(r) = -\frac{i2\pi e^2 MN\eta}{\beta^2 E_0 T_0^2 \omega_s}\frac{m}{r}\frac{dg_0}{dr}\int r'dr' R_m(r')\sum_q \frac{Z_0^{\parallel}(\omega_q)}{\omega_q} J_m(\omega_q r') J_m(\omega_q r) \ . \tag{8.27}$$

The spread in synchrotron frequency can be introduced by letting ω_s be a function of r. Moving the factor $\Omega - m\omega_s(r)$ to the right side, the radial distribution R_m can be eliminated by multiplying both sides by $rJ_m(r)$ and integrating over dr. We then arrive at the dispersion relation,

$$1 = -\frac{i2\pi e^2 MNm\eta}{\beta^2 E_0 T_0^2 \omega_s}\sum_q \frac{Z_0^{\parallel}(\omega_q)}{\omega_q}\int dr\,\frac{dg_0}{dr}\frac{J_m^2(\omega_q r)}{\Omega - m\omega_s(r)} \ . \tag{8.28}$$

Stability and growth contours can be derived from the dispersion relation of Eq. (8.28) in just the same way as in the discussion of microwave instability for a single bunch.

8.1.1 WATER BAG MODEL

When the spread in synchrotron frequency is small, Eq. (8.28) gives the frequency shift

$$\Omega - m\omega_s = \frac{i2\pi e^2 MNm\eta}{\beta^2 E_0 T_0^2 \omega_s} \sum_q \frac{Z_0^{\parallel}(\omega_q)}{\omega_q} \left[- \int dr \, \frac{dg_0}{dr} J_m^2(\omega_q r) \right] \ , \tag{8.29}$$

where the expression inside the square brackets can be viewed as a distribution dependent form factor, which is positive definite because dg_0/dr is negative. Take the simple case of a single bunch of length $2\hat{\tau}$ and uniform distribution in the longitudinal phase space, which is usually called the *water bag model*. Then

$$g_0(r) = \frac{1}{\pi \hat{\tau}^2} \, H(\hat{\tau} - r) \ , \tag{8.30}$$

where the Heaviside function is defined as $H(x) = 1$ when $x > 0$ and zero otherwise. The form factor becomes

$$F = \frac{1}{\pi \hat{\tau}^2} \, J_m^2(\omega_q \hat{\tau}) \approx \frac{\omega_q^2}{4\pi} \frac{1}{(m!)^2} \left(\frac{\omega_q \hat{\tau}}{2} \right)^{2m-2} \ , \tag{8.31}$$

where the assumption of a short bunch has been made in the last step. The growth rate driven by the impedance can now be written as

$$\frac{1}{\tau_m} = \frac{e^2 N \eta}{2\beta^2 E_0 T_0^2 \omega_s} \frac{m}{(m!)^2} \sum_q \left(\frac{\omega_q \hat{\tau}}{2} \right)^{2m-2} \omega_q \, \mathcal{R}e \, Z_0^{\parallel}(\omega_q) \ , \tag{8.32}$$

where, for one bunch, $\omega_q = q\omega_0 + \Omega$.

8.1.2 ROBINSON INSTABILITY

The $m = 0$ mode is a trivial mode which gives $\Omega_0 = 0$. It describes the potential-well distortion mode addressed in Chapter 4 and is of not much interest here where the emphasis is on instabilities. The next azimuthal mode is $m = 1$ which describes dipole oscillations and we expect $\Omega \approx \omega_s$. Consider the situation of having the driving impedance as a resonance so narrow that there is only one $q > 0$ that satisfies

$$\omega_r \approx q\omega_0 \pm \omega_s \ , \tag{8.33}$$

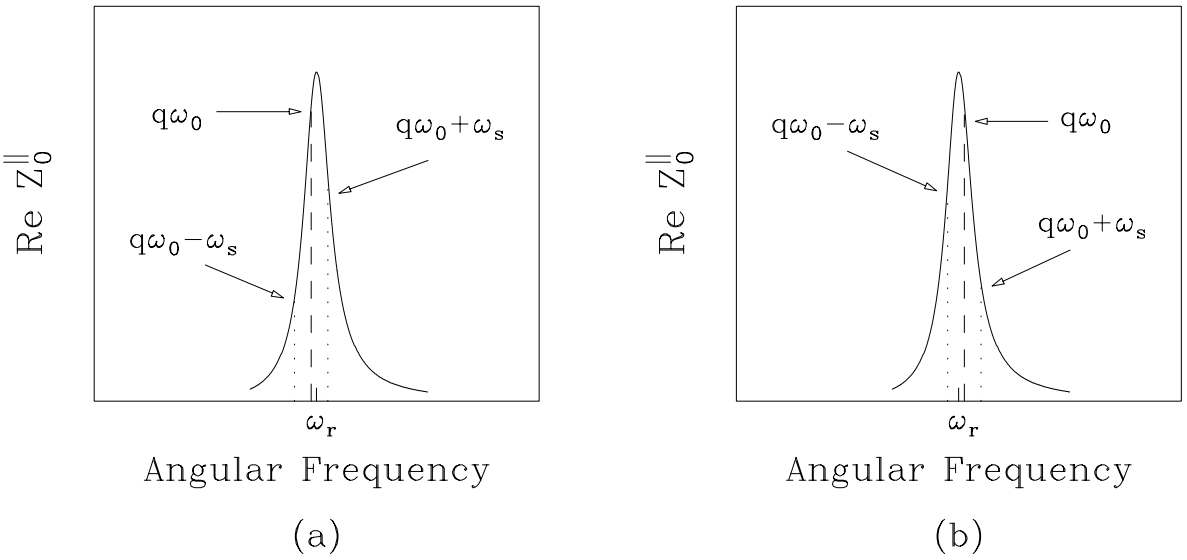

Figure 8.1: (a) Above transition, if the resonant frequency ω_r is slightly above a revolution harmonic $q\omega_0$, $\mathcal{R}e\, Z_0^{\|}$ at the upper synchrotron side-band is larger than at the lower synchrotron side-band. The system is unstable. (b) Above transition, if ω_r is slightly below a harmonic line, $\mathcal{R}e\, Z_0^{\|}$ at the upper side-band is smaller than at the lower side-band, and the system is stable.

where $\omega_r/(2\pi)$ is the resonant frequency. The growth rate can therefore be expressed as

$$\frac{1}{\tau_1} = \mathcal{I}m\,\Delta\omega_s = \frac{\eta e^2 N\omega_r}{2\beta^2 E_0 T_0^2 \omega_s}[\mathcal{R}e\, Z_0^{\|}(q\omega_0+\omega_s) - \mathcal{R}e\, Z_0^{\|}(q\omega_0-\omega_s)]\ , \tag{8.34}$$

where the first term corresponds to positive frequency and the second negative frequency. If the resonant frequency is slightly above $q\omega_0$ as illustrated in Fig. 8.1(a), we have $\mathcal{R}e\, Z_0^{\|}(q\omega_0+\omega_s) > \mathcal{R}e\, Z_0^{\|}(q\omega_0-\omega_s)$. Above transition, the growth rate will be positive or there is instability. On the other hand if $\omega_r < q\omega_0$ as illustrated in Fig. 8.1(b), the growth rate is negative and the system is damped. This instability criterion was first analyzed by Robinson [1]. Note that the growth rate of Eq. (8.34) is independent of the bunch length when the bunch is short, implying that for the dipole mode, this is a point-bunch theory. More about Robinson stability criterion was discussed in Chapter 7.

For M equal bunches, Eq. (8.34) becomes, for coupled-bunch mode μ,

$$\frac{1}{\tau_{1\mu}} = \frac{\eta e^2 NM\omega_r}{2\beta^2 E_0 T_0^2 \omega_s}[\mathcal{R}e\, Z_0^{\|}(qM\omega_0+\mu\omega_0+\omega_s) - \mathcal{R}e\, Z_0^{\|}(q'M\omega_0-\mu\omega_0-\omega_s)]\ . \tag{8.35}$$

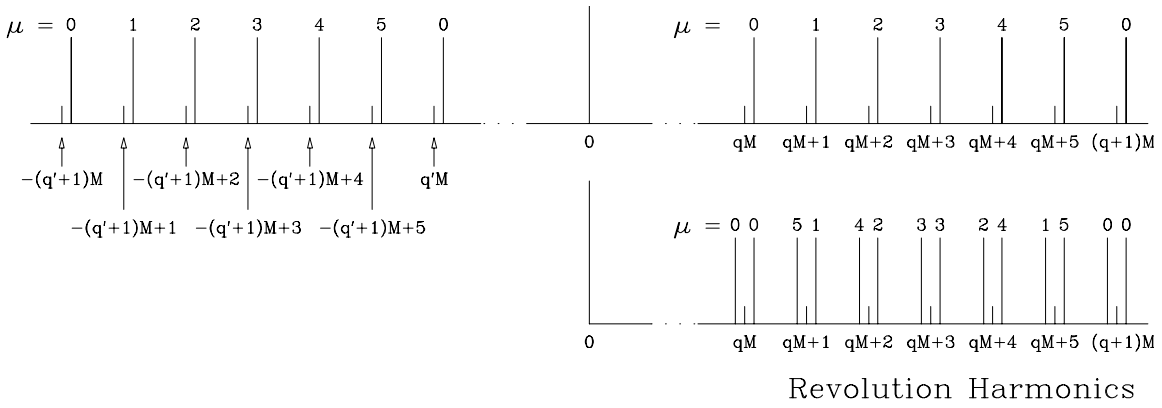

Figure 8.2: Top plot shows the synchrotron lines for both positive and negative revolution harmonics for the situation of $M = 6$ identical equally-spaced bunches. The coupled-bunch modes $\mu = 0$, 1, 2, 3, 4, 5 are listed at the top of the synchrotron lines. Lower plot shows the negative-harmonic side folded onto the positive-harmonic side. We see upper and lower side-band for each harmonic line.

When $\mu = 0$, both terms will contribute with $q' = q$ and we have exactly the same Robinson's stability or instability as for the single bunch situation. This is illustrated in Fig. 8.2. When $\mu = M/2$ if M is even, both terms will contribute with $q' = q$, and the same Robinson's stability or instability will apply. For the other $M-2$ modes, only one term will be at or close to the resonant frequency and only one term will contribute. If the positive-frequency term contributes, we have instability. If the negative-frequency term contributes, we have damping instead. If one choose to speak in the language of only positive frequencies, there will be an upper and lower synchrotron side-band surrounding each revolution harmonic. Above transition, the coupled-bunch system will be unstable if the driving resonance leans towards the upper side-band and stable if it leans towards the lower side-band.

For the higher azimuthal modes ($m > 1$) driven by a narrow resonance, we have the same Robinson instability. The growth rates are

$$\frac{1}{\tau_{m\mu}} = \frac{\eta e^2 N M \omega_r}{2\beta^2 E_0 T_0^2 \omega_s} \frac{m}{(m!)^2} \left(\frac{\omega_r \hat{\tau}}{2}\right)^{2m-2} \left[\mathcal{R}e\, Z_0^{\parallel}(qM\omega_0 + \mu\omega_0 + \omega_s) - \mathcal{R}e\, Z_0^{\parallel}(q'M\omega_0 - \mu\omega_0 - \omega_s)\right] , \tag{8.36}$$

which depend on the bunch length as $\hat{\tau}^{2m-2}$. As a result, higher azimuthal instabilities for short bunches will be much more difficult to excite.

Landau damping can come from the spread of the synchrotron frequency. The

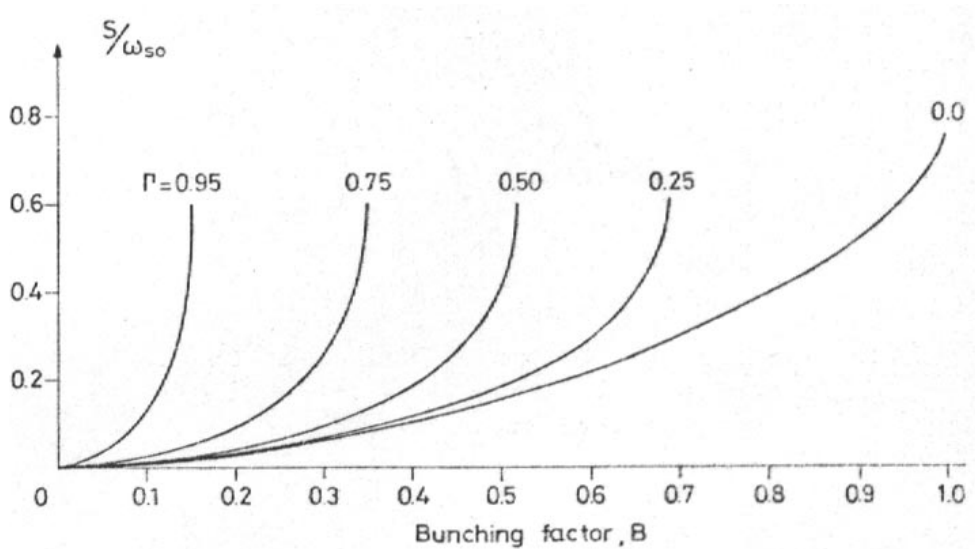

Figure 8.3: Synchrotron frequency spread S as a function of single-bucket bunching factor $B \approx \tau_L f_0$ for various values of $\Gamma = \sin\phi_s$. τ_L is full bunch length, f_0 is revolution frequency, ϕ_s is synchronous angle, and ω_{s0} is unperturbed angular synchrotron frequency.

spread due to the nonlinear sinusoidal rf wave form can be written as (Exercise 8.3)

$$\frac{\Delta\omega_s}{\omega_s} = \left(\frac{\pi^2}{16}\right)\left(\frac{1+\sin^2\phi_s}{1-\sin^2\phi_s}\right)(h\tau_L f_0)^2 \ , \tag{8.37}$$

where τ_L is the total length of the bunch and ϕ_s is the synchronous angle, and is valid for small amplitudes. The mode will be stable if [2]

$$\frac{1}{\tau} \lesssim \frac{\sqrt{m}}{4}\Delta\omega_s \ . \tag{8.38}$$

When the synchronous angle $\phi_s \neq 0$, the computation of synchrotron frequency spread is tedious. A numerical calculation is shown in Fig. 8.3 for various $\Gamma = \sin\phi_s$. The expression in Eq. (8.37) comes from a fitting to the numerical calculation at small amplitudes.

8.2 TIME DOMAIN

The longitudinal coupled-bunch instabilities can also be studied without going into the frequency domain. We are employing the same Vlasov equation in Eq. (8.7), but using the wake function of a resonance in the time domain [2].

The wake function for a resonance with resonant frequency $\omega_r/(2\pi)$, shunt impedance R_s and quality factor Q was given in Eq. (1.40). For a narrow resonance with $\alpha = \omega_r/(2Q) \ll \omega_r$, we can neglect the sine term[‡] and simplify the wake function to

$$W_0'(z) = \frac{\omega_r R_s}{Q}\, e^{-\alpha z/v} \cos\frac{\omega_r z}{v} \qquad \text{when } z > 0\ . \tag{8.39}$$

The wake force is then given by

$$\langle F_0^{\parallel}(\tau; s)\rangle = -\frac{e^2\omega_r R_s}{QC}\int_{\tau}^{\infty} d\tau'\, e^{-\alpha(\tau'-\tau)} \cos[\omega_r(\tau'-\tau)]\, \rho\,[\tau'; s - v(\tau'-\tau)]\ . \tag{8.40}$$

Now let $\rho(\tau; s)$ represent the line density of the individual bunch, which has a phase lead of $2\pi\mu/M$ for mode μ compared with the preceding bunch $\tau_{\rm sep} = T_0/M$ ahead, and is influenced by all the preceding bunches. The location argument s of ρ in Eq. (8.40) becomes[§] $s - k\tau_{\rm sep} - v(\tau'-\tau)$, with $k = 0,\ 1,\ 2,\ \cdots$. For simplicity, we neglect the time delay $\tau'-\tau$. In the time variation $e^{-i\Omega s/v}$ where $\Omega \approx m\omega_s$, this delay causes a phase delay $\Omega(\tau'-\tau)$ which is negligible in comparison with the phase change due to the resonator. We will also neglect the variation in the attenuation factor over one bunch in $e^{-\alpha(\tau'-\tau)}$. Then the wake force exerted on a particle in the μ-th coupled-bunch mode can be written as

$$\langle F_{0\mu}^{\parallel}(\tau; s)\rangle = -\frac{e^2\omega_r R_s}{QC}\sum_{k=0}^{\infty} e^{2\pi i k\mu/M - k\alpha\tau_{\rm sep}} \int_{\text{one bunch}} d\tau' \cos[\omega_r(\tau'-\tau+k\tau_{\rm sep})]\, \rho_1(\tau') e^{-i\Omega(s/v - k\tau_{\rm sep})}\ . \tag{8.41}$$

It is worth pointing out that the lower limits of the summation and integration *cannot* be extended to $-\infty$ as before, because the explicit expression of the wake function has been used. Note that only the perturbed line density ρ_1 is included. This is because the unperturbed part ρ_0 should have been taken care of in the potential-well distortion consideration. Changing the integration variables from $(\tau, \Delta E)$ to (r, ϕ) while keeping only the azimuthal m,

$$\rho_1(\tau')d\tau' = \alpha_m R_m(r') e^{im\phi'} d\tau' d\Delta E' = \frac{E_0\omega_s\beta^2}{\eta}\, \alpha_m R_m(r') e^{im\phi'} r' dr' d\phi'\ . \tag{8.42}$$

[‡]The sine term can be included at the expense of a slightly more complicated derivation.

[§]Here we include the term $k\tau_{\rm sep}$ which Sacherer had left out. This term is important to exhibit Robinson's criterion of phase stability.

Substituting the wake force into Eq. (8.7), we arrive at

$$(\Omega - m\omega_s)R_m(r) = \frac{ie^2N\eta\omega_r R_s}{2\pi\beta^2 E_0 Q T_0 \omega_s}\frac{dg_0}{dr}\sum_{k=0}^{\infty} e^{2\pi ik\mu/M - k(\alpha - i\Omega)\tau_{\rm sep}}\times$$
$$\times \int_0^\infty r'dr' R_m(r')\int_{-\pi}^{\pi} d\phi\, e^{-im\phi}\sin\phi\int_{-\pi}^{\pi} d\phi' e^{im\phi'}\cos[\omega_r(r'\cos\phi' - r\cos\phi + k\tau_{\rm sep})]\ , \quad (8.43)$$

where again we have used the unperturbed distribution $g_0(r)$ given by Eq.(8.26) which is normalized to unity. The result is

$$(\Omega - m\omega_s)R_m(r) = -\frac{2\pi e^2 N R_s m\eta}{\beta^2 E_0 Q T_0 \omega_s}\frac{dg_0}{dr}\times$$
$$\times\sum_{k=0}^{\infty} e^{2\pi ik\mu/M - k(\alpha - i\Omega)\tau_{\rm sep}}\sin(k\omega_r\tau_{\rm sep})\int_0^\infty dr' R_m(r')\frac{r' J_m(\omega_r r')J_m(\omega_r r)}{r}\ . \quad (8.44)$$

Finally, we introduce Landau damping by allowing the synchrotron frequency to be a function of the radial distance from the center of the bunch in the longitudinal phase phase. Moving $\Omega - m\omega_s(r)$ to the right side and performing an integration over rdr, we can eliminate R_m and obtain the dispersion relation

$$1 = -\frac{i2\pi e^2 MNm\eta R_s}{\beta^2 E_0 T_0^2 \omega_s\omega_r} D(\alpha\tau_{\rm sep})\int_0^\infty dr\frac{dg_0}{dr}\frac{J_m^2(\omega_r r)}{\Omega - m\omega_s(r)}\ , \quad (8.45)$$

where we have defined the function[¶]

$$D(\alpha\tau_{\rm sep}) = -i2\alpha\tau_{\rm sep}\sum_{k=0}^{\infty} e^{2\pi ik\mu/M - k(\alpha - i\Omega)\tau_{\rm sep}}\sin k\omega_r\tau_{\rm sep}\ , \quad (8.46)$$

which contains all the information about the quality factor of the resonance and its location with respect to the revolution harmonics. It is interesting to note that Eq. (8.45) closely resembles Eq. (8.28). It will be shown below that $D = 1$ for a narrow resonance with the resonant peak located at $(qM+\mu)\omega_0 + m\omega_s$. Thus the two dispersion relations are identical. In fact, they are the same even when the resonant peak is not exactly located at a synchrotron line.

Now let us study the function $D(\alpha\tau_{\rm sep})$. Noting that the bunch separation is $\tau_{\rm sep} = T_0/M$, this function can be rewritten as

$$D(\alpha\tau_{\rm sep}) = \alpha\tau_{\rm sep}\left(\frac{1}{1-e^{x_+}} - \frac{1}{1-e^{x_-}}\right)\ , \quad (8.47)$$

[¶]We would like $D = \pm 1$ when the resonance is at the upper/lower side-band. As a result, our definition of D differs from Sacherer's by a phase.

where

$$x_\pm = \frac{2\pi i}{M}\left(q_\pm M + \mu + m\frac{\omega_s}{\omega_0} \mp \frac{\omega_r}{\omega_0}\right) - \alpha\tau_{\rm sep} \ . \tag{8.48}$$

The $q_\pm M$ term comes about because we can replace μ in Eq. (8.46) by $q_\pm M+\mu$, where $q_\pm$ are positive/negative integers and $\mu = 0,\ 1,\ \cdots,\ M-1$. When the resonance is extremely narrow, we have $\alpha\tau_{\rm sep} = \omega_r\tau_{\rm sep}/(2Q) \ll 1$. The two terms in Eq. (8.47) almost cancel each other so that $D(\alpha\tau_{\rm sep}) \approx 0$ unless $\omega_r \approx (|q_\pm|M\pm\mu)\omega_0$. For modes $\mu \neq 0$ and $\mu \neq \frac{1}{2}M$ if M is even, only one of the two terms in Eq. (8.47) contributes. If $\omega_r \approx (|q_\pm|M\pm\mu)\omega_0 \pm m\omega_s$, we have $|x_+| \ll 1$ or $|x_-| \ll 1$ and

$$D(\alpha\tau_{\rm sep}) \approx \mp\frac{\alpha\tau_{\rm sep}}{x_\pm} = \frac{-i\omega_r/(2Q)}{\omega_r - [(|q_\pm|M\pm\mu)\omega_0 \pm m\omega_s] \mp i\omega_r/(2Q)} \approx \pm 1 \ . \tag{8.49}$$

When $\mu = 0$ or $\mu = M/2$ if M is even, it is possible to choose q_+ and q_- so that both terms will contribute. We have

$$D \approx \frac{-i\omega_r/(2Q)}{\omega_r - [(q_+M+\mu)\omega_0 + m\omega_s] - i\omega_r/(2Q)} + \frac{-i\omega_r/(2Q)}{\omega_r - [(|q_-|M-\mu)\omega_0 - m\omega_s] + i\omega_r/(2Q)} \ , \tag{8.50}$$

where $q_+ = |q_-|$ for $\mu = 0$ and $|q_-| = q_+ + 1$ for $\mu = M/2$. Note that Eq. (8.50) is just proportional to $[Z_0^\parallel(q_+M\omega_0 + \mu\omega_0 + m\omega_s + i\alpha) - Z_0^\parallel(|q_-|M\omega_0 - \mu\omega_0 - m\omega_s - i\alpha)]$, and we recover the Robinson's stability criterion derived in Eq. (8.35).

On the other hand, when the resonance is broad, $\alpha\tau_{\rm sep} \gg 1$. The $k = 1$ in Eq. (8.46) dominates since $k = 0$ does not contribute and we have instead

$$D(\alpha\tau_{\rm sep}) \approx -i2\alpha\tau_{\rm sep}\sin(\omega_r\tau_{\rm sep})e^{2\pi i\mu/M - \alpha\tau_{\rm sep}} \ . \tag{8.51}$$

Therefore coupled-bunch modes near $\mu = \pm\frac{1}{4}M$ are most strongly excited, although $|D|$ will be much less than unity. Figure 8.4 plots $|D|$ versus ω_r/ω_0 for the situation of $M = 10$ bunches. The solid lines show $|D| \approx 1$ for narrow resonance. The dotted curve are for broad-band resonance when the bunch to bunch attenuation decrement is $\alpha\tau_{\rm sep} = 4$; the values of $|D|$ are small and appear to be mode-independent. The dashed curves correspond the intermediate case with bunch-to-bunch attenuation decrement $\alpha\tau_{\rm sep} = 1$. From left to right, they are for modes $\mu = 0$, 1 and 9, 2 and 8, 3 and 7, 4 and 6, 5. We see that $|D|_{\rm max}$ is roughly the same for each mode. Note that $\alpha\tau_{\rm sep} = 1$ translates into $(\Delta\omega_r/\omega_0)_{\rm FWHM} = M/\pi = 3.2$ or the resonance covers more than 3 revolution harmonics. It is demonstrated in the figure that all modes will not be excited if the ω_r/ω_0 falls exactly on qM or $q(\frac{1}{2}M)$ if M is even. This is because

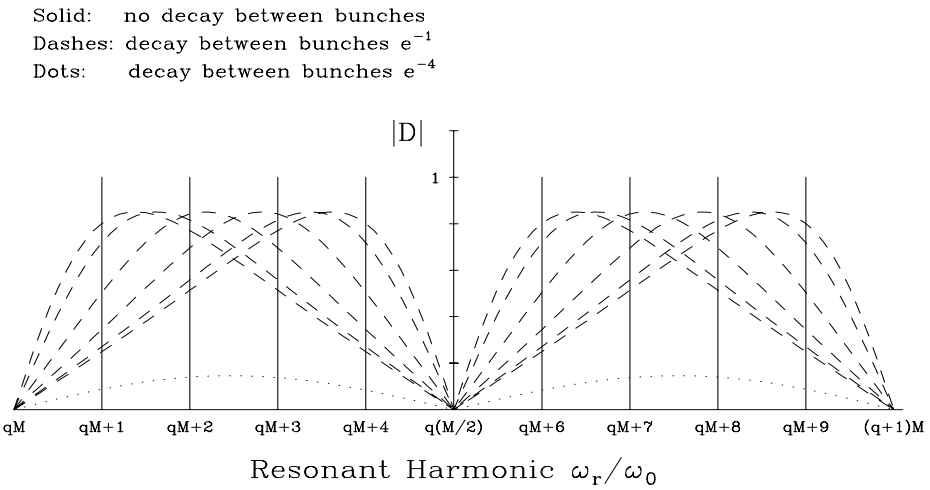

Figure 8.4: $|D|$ as functions of resonant harmonic ω_r/ω_0 for $M = 10$ bunches when bunch-to-bunch decay decrement $\alpha\tau_{\rm sep} \ll 1$ for narrow-band resonance (solid), $\alpha\tau_{\rm sep} = 4$ for broad-band resonance (dots), and $\alpha\tau_{\rm sep} = 1$ for resonance in between (dashes). The dashed curves from left to right represent coupled-bunch modes $\mu = 0$, 1 and 9, 2 and 8, 3 and 7, 4 and 6, 5. The excitations at $\omega_r/\omega_0 = 0$, or $M/2$ is always zero, because we have set the synchrotron frequency to zero in the plot.

in drawing the plot, the limit $\omega_s \to 0$ has been taken. Figure 8.5 plots $|D|_{\rm max}$ versus the bunch-to-bunch decrement $\alpha\tau_{\rm sep}$, showing that it is less than 5% from unity when $\alpha\tau_{\rm sep} < 0.55$.

In the event that the spread in synchrotron frequency is small, we can obtain from Eq. (8.45) the synchrotron frequency shift

$$\Omega - m\omega_s = -\frac{i2\pi e^2 N R_s m M \eta}{\beta^2 E_0 \omega_s \omega_r T_0^2} D(\alpha\tau_{\rm sep}) \int_0^\infty dr \frac{dg_0}{dr} J_m^2(\omega_r r) \ , \tag{8.52}$$

where the integral can be viewed as a form factor which is distribution dependent. A dimensionless form factor

$$F_m(\Delta\phi) = -\frac{4\pi m\hat{\tau}}{\omega_r} \int_0^\infty dr \frac{dg_0}{dr} J_m^2(\omega_r r) \tag{8.53}$$

can now be defined for each azimuthal, where $\hat{\tau}$ is the half bunch length and $\Delta\phi = 2\omega_r\hat{\tau}$ is the change in phase of the resonator during the passage of the whole bunch. Then the frequency shift can be rewritten as

$$\Omega - m\omega_s = \frac{i\eta e^2 N M R_s}{4\pi\beta^2 E_0 \nu_s T_0 \hat{\tau}} D(\alpha\tau_0) F_m(\Delta\phi) \ , \tag{8.54}$$

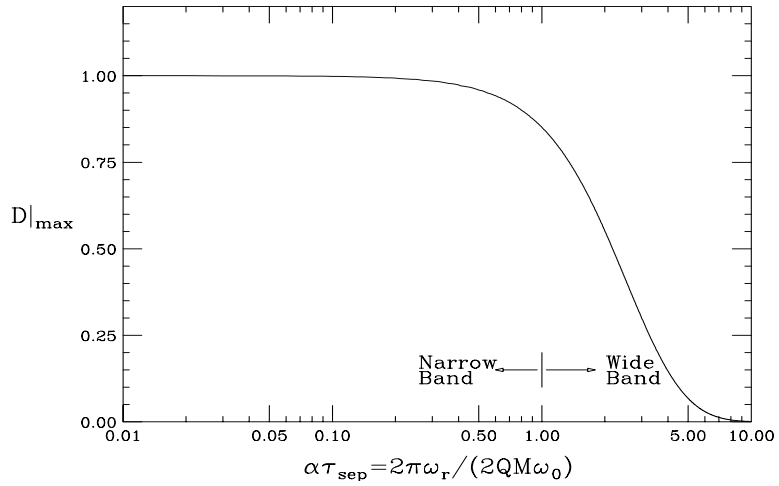

Figure 8.5: $|D|_{\max}$ as a function of bunch-to-bunch decay decrement $\alpha\tau_{\rm sep}$. Note that $|D|_{\max} \approx 1$ for narrow resonances but drops very rapidly as the resonance becomes broader.

where $\nu_s = \omega_s/\omega_0$ is the synchrotron tune.

We take as an example the *parabolic* distribution in the longitudinal phase space,[‖] which implies

$$g_0(r) = \frac{2}{\pi\hat{\tau}^4}(\hat{\tau}^2 - r^2) \qquad \text{and} \qquad \frac{dg_0}{dr} = -\frac{4r}{\pi\hat{\tau}^4} \ . \tag{8.55}$$

The form factor is

$$\begin{aligned} F_m(\Delta\phi) &= \frac{32m}{\Delta\phi}\int_0^1 J_m^2(\tfrac{1}{2}\Delta\phi\, x)x\,dx \\ &= \frac{16m}{\Delta\phi}\left[J_m^2(\tfrac{1}{2}\Delta\phi) - J_{m+1}(\tfrac{1}{2}\Delta\phi)J_{m-1}(\tfrac{1}{2}\Delta\phi)\right] \ , \end{aligned} \tag{8.56}$$

which is plotted in Fig. 8.6 for $m = 1$ to 6. The form factor specifies the efficiency with which the resonator can drive a given mode. We see that the maximum value of F_1 for the dipole mode occurs when $\Delta\phi \approx \pi$. This is to be expected because the head and tail of the bunch will be driven in opposite directions. Similarly, the quadrupole or breathing mode is most efficiently driven when $\Delta\phi \approx 2\pi$, and so on for the higher modes. In general, mode m is most efficiently driven when the resonator frequency is $\Delta\phi \approx m\pi$. Note also that the maximum value of F_m drops faster than $m^{-1/2}$, implying that higher azimuthal modes are harder to excite. For distributions other than the

[‖]This is different from the so-called parabolic distribution, which is actually parabolic line density.

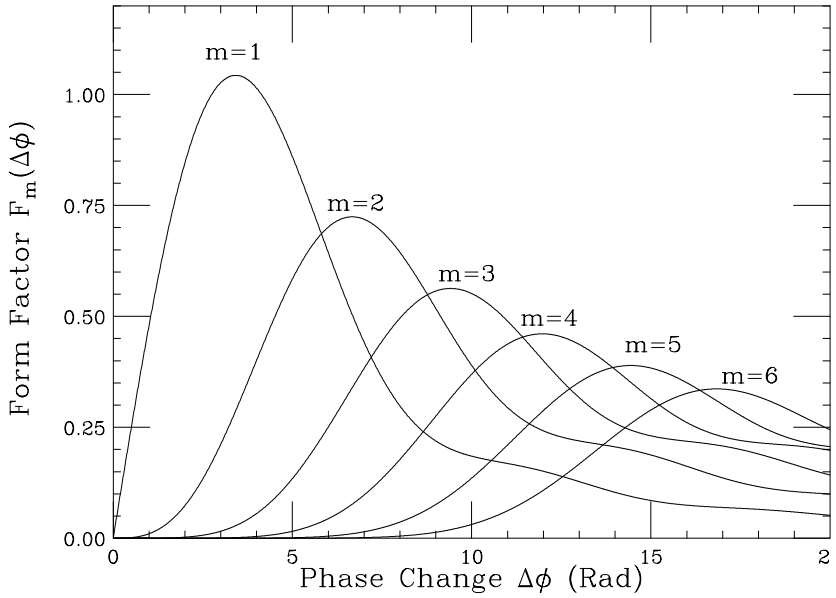

Figure 8.6: Sacherer form factor for longitudinal oscillation inside a bunch with azimuthal modes $m = 1,\ 2,\ 3,\ 4,\ 5$ and 6. The unperturbed parabolic distribution in the longitudinal phase space is assumed.

"parabolic" of Eq. (8.55), we expect form factors to have similar properties. However, a shorter bunch does not necessarily imply a slower growth especially for the $m = 1$ mode, although the excitation in the form factor $F_m(\Delta\phi)$ is small. According to Eq. (8.54), the growth rate is obtained from multiplying the form factor $F_m(\Delta\phi)$ with $eN/\hat{\tau}$, the local linear charge density or peak current. In fact, with a fixed number of particles in the bunch, as the bunch length is shortened, the local linear charge density increases, thus enhancing the growth rate. As a result, a more practical form factor should be $\bar{F}_m(\Delta\phi) = 2F_m(\Delta\phi)/\Delta\phi$ as plotted in Fig. 8.7 in logarithmic scale. It is clear that for small $\Delta\phi$, $F_1 \approx \frac{1}{2}\Delta\phi$ and $\bar{F}_1 \approx 1$. From Eq. (8.52), the growth rate for the dipole mode above transition can be written as

$$\frac{\eta e^2 N M R_s \omega_r}{2\beta^2 E_0 \omega_s T_0^2}\ , \tag{8.57}$$

which agrees with the expression in Eq. (8.35) derived for short bunches. It is also evident from Fig. 8.7 that the excitations of higher azimuthal modes will be very much smaller.

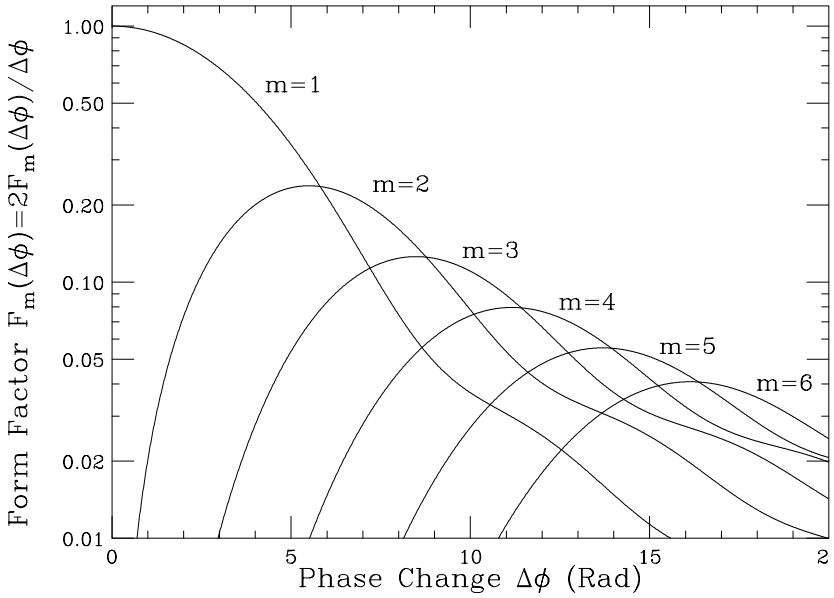

Figure 8.7: A more useful form factor $\bar{F}(\Delta\phi)$ in logarithmic scale for longitudinal oscillation inside a bunch with azimuthal modes $m = 1,\ 2,\ 3,\ 4,\ 5$ and 6. The unperturbed parabolic distribution in the longitudinal phase space is assumed. It is related to the Sacherer's form factor of Fig. 8.6 by $\bar{F}(\Delta\phi) = 2F(\Delta\phi)/\Delta\phi$.

8.3 OBSERVATION AND CURES

The easiest way to observe longitudinal coupled-bunch instability is in mountain-range plot, where bunches oscillate in a particular pattern as time advances. Examples are shown in Figs. 8.8 and 8.9. Streak camera can also be used to capture the phases of adjacent bunches as a function of time. From the pattern of coupling, the coupled-mode μ can be determined. From the frequency of oscillation, the azimuthal mode m can also be determined. Then we can pin down the frequency $\omega_r/(2\pi)$ of the offending resonance driving the instability.

Observation can also be made in the frequency domain by zooming in the region between two rf harmonics in the way illustrated in Fig. 8.2. The coupled-bunch mode excited will be shown as a strong spectral line in between.

Longitudinal coupled-bunch instability will lead to an increase in bunch length and an increase in energy spread. For a light source, this translates into an increase in the spot size of the synchrotron light.

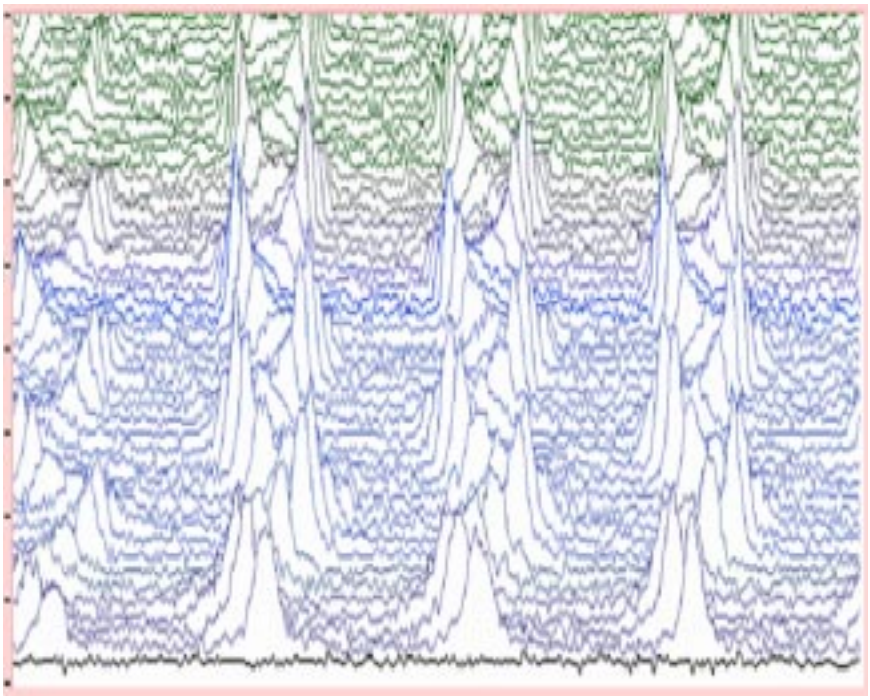

Figure 8.8: (color) Mountain-range plot showing coupled-bunch instability in the Fermilab Main Injector just after injection at 8 GeV.

There are many way to cure longitudinal coupled bunch instability. The driving resonances are often the higher order modes inside the rf cavities. When the particular resonance is identified and if it is much narrower than the revolution frequency of the ring, we can try to shift its frequency so that it resides in between two revolution harmonics and becomes invisible to the beam particles. We can also study the electromagnetic field pattern of this resonance mode inside the cavity and install passive resistors and antennae to damp this particular mode. This method has been used widely in the Fermilab Booster, where longitudinal coupled-bunch instability had been very severe after the beam passed the transition energy. At that time, the bunch area increased almost linearly with bunch intensity. Passive damping of several offending modes cured this instability to such a point that the bunch area does not increase with bunch intensity anymore.

Longitudinal coupled-bunch instability had also been observed in the former Fermilab Main Ring. Besides passive damping of the cavity resonant modes, the instability was also reduced by lowering the rf voltage. Lowering the rf voltage will lengthen the bunch and reduce the form factor F. This is only possible for a proton machine where

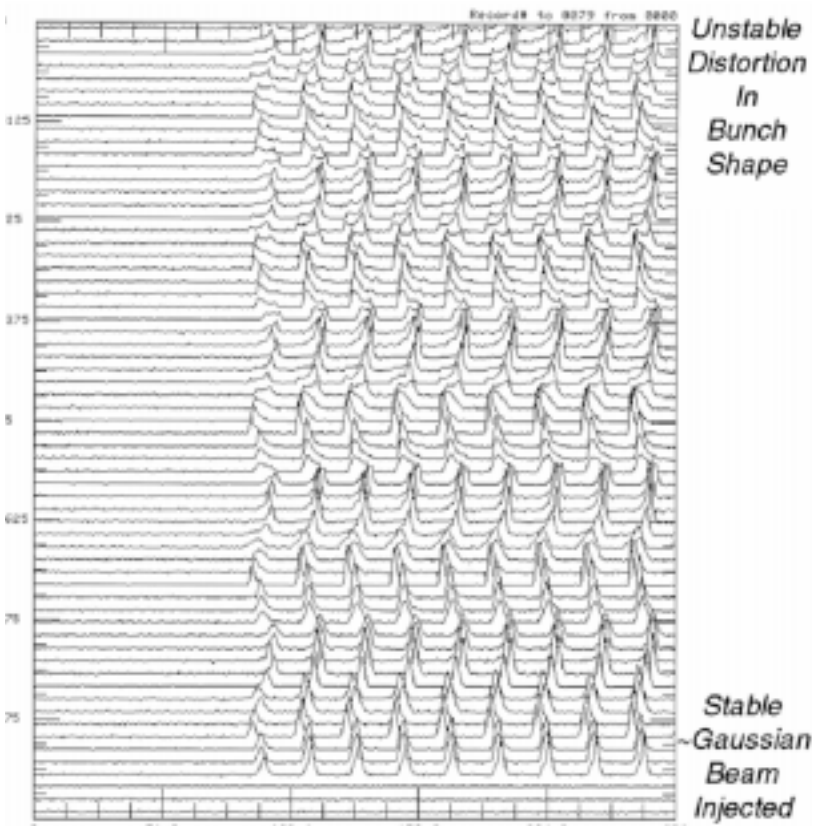

Figure 8.9: Mountain range plot showing bunches in a batch executing coupled-bunch instability in the Fermilab Main Injector just after injection at 8 GeV

the bunches are long. It will not work for the short electron bunches for the $m = 1$ dipole mode. This is because, as mentioned before, the form factor for the dipole mode is not sensitive to the bunch length for short bunches. Even for a proton machine, the rf voltage cannot be reduced by a large amount because proton bunches are usually rather tight inside the rf bucket, especially during ramping.

If the growth turns out to be harmful, a fast bunch-by-bunch damper may be necessary to damp the dipole mode ($m = 1$). A damper for the quadrupole mode ($m = 2$) may also be necessary. This consists essentially of a wall-gap pickup monitoring the changes in bunch length and the corresponding excitation of a modulation of the rf waveform with roughly twice the synchrotron frequency. A feed-back correction is then made to the rf voltage. Another way to damp the longitudinal coupled-bunch instability is to break the symmetry between the M bunches. For example, a 5% to 10% variation in the intensity of the bunches will help. Also the bunches are usually

not placed symmetrically in the ring. Some analysis shows that the stability will be improved if some bunches in the symmetric configuration are missing.

There can also be Landau damping, which comes from the spread of the synchrotron frequency. The spread due to the nonlinear sinusoidal rf wave form as given by Eq. (8.37 is usually small unless the synchronous angle is large. Electron bunches are usually much smaller in size than the rf bucket. As a result the spread in synchrotron frequency will be very minimal, and does not help much in Landau damping.

8.3.1 HIGHER-HARMONIC CAVITIES

In order to Landau damp longitudinal coupled-bunch instability, a large spread in synchrotron frequency inside the bunch is required. One way to do this is to install a higher-harmonic cavity, sometime known as *Landau cavity* [3]. For example, the higher-harmonic cavity has resonant frequency $m\omega_{\rm rf}$, where $\omega_{\rm rf}$ is the resonant frequency of the fundamental rf cavity. The total rf voltage seen by the beam particles becomes

$$V(\tau) = V_{\rm rf}\big[\sin(\phi_s - \omega_{\rm rf}\tau) - r\sin(\phi_m - m\omega_{\rm rf}\tau)\big] - \frac{U_s}{e} \ , \tag{8.58}$$

where the phase angle ϕ_s is to compensate for the U_s, the radiation energy loss or any required acceleration. We would like the bottom of the potential well, which is the integral of $V(\tau)$, to be as flat as possible. The rf voltage seen by the synchronous particle is compensated to zero by the energy lost to synchrotron radiation. In addition, we further require

$$\left.\frac{\partial V}{\partial \tau}\right|_{\tau=0} = 0 \ , \qquad \text{and} \qquad \left.\frac{\partial^2 V}{\partial \tau^2}\right|_{\tau=0} = 0 \ , \tag{8.59}$$

so that the potential will become quartic instead. We therefore have 3 equations in 3 unknowns:

$$\begin{cases} \sin\phi_s = r\sin\phi_m + \dfrac{U_s}{eV_{\rm rf}} \ , \\ \cos\phi_s = rm\cos\phi_m \ , \\ \sin\phi_s = rm^2\sin\phi_m \ , \end{cases} \tag{8.60}$$

from which ϕ_m and k can be solved easily (Exercise 8.4). For small amplitude oscillation, the potential becomes

$$-\int V(\tau)d(\omega_{\rm rf}\tau) \longrightarrow \frac{m^2-1}{24}(\omega_{\rm rf}\tau)^4 V_{\rm rf}\cos\phi_s \ , \tag{8.61}$$

which is quartic and the synchrotron frequency is (Exercise 8.5)

$$\frac{\omega_s(\tau)}{\omega_{s0}} = \frac{\pi}{2}\left(\frac{m^2-1}{6}\right)^{1/2} \frac{\omega_{\rm rf}\tau}{K(1/\sqrt{2})} \left[\frac{1-\left(\dfrac{m^2}{m^2-1}\,\dfrac{U_s}{eV_{\rm rf}}\right)^2}{1-\left(\dfrac{U_s}{eV_{\rm rf}}\right)^2}\right]^{1/4}, \tag{8.62}$$

where the last factor can usually be neglected; its deviates from unity by only $\sim [(m^2-1)U_s/(2eV_{\rm rf})]^2$ if the synchronous angle is small. In above, ω_{s0} is the synchrotron frequency at zero amplitude when the higher-harmonic cavity voltage is turned off, and $K(1/\sqrt{2}) = 1.854$ is the complete elliptic integral of the first kind which is defined as

$$K(t) = \int_0^{\pi/2} \frac{d\theta}{\sqrt{1-t^2\sin^2\theta}}\ . \tag{8.63}$$

We see that the synchrotron frequency is zero at zero amplitude and increases linearly with amplitude. This large spread in synchrotron frequency may be able to supply ample Landau damping to the longitudinal coupled-bunch instability.

In the situation where there is no radiation loss and no acceleration, $U_s = 0$, the solution of Eq. (8.60)simplifies, giving $\phi_s = \phi_m = 0$ and the ratio of the voltages of higher-harmonic cavity to the fundamental $r = 1/m$. Of course, it is also possible to have $r \neq 1/m$. Then the synchrotron frequency at the zero amplitude will not be zero and the spread in synchrotron frequency can still be appreciable. When $m = 2$, i.e., having a second harmonic cavity, the mathematics simplifies. The synchrotron frequencies for various values of r are plotted in Fig. 8.10. Here, $r = 0$ implies having only the fundamental rf while $r = \frac{1}{2}$ the situation of having the synchrotron frequency linear in amplitude for small amplitudes. In between, the synchrotron frequency spread decreases as r decreases. Notice that for $0.3 \lesssim r < 0.5$, the synchrotron frequency has a maximum near the rf phase of $\sim 100°$. Particles near there will have no Landau damping at all and experience instability. Thus the size of the bunch is limited when a double cavity is used. Also the size of the bunch cannot be too small because of two reasons: first, the average synchrotron frequency may have been too low, and second, the central region of the phase space is a sea of chaos [5].

A Landau cavity increases the spread in synchrotron frequency, therefore it is ideal in damping mode-mixing instability and coupled-bunch instability. However, it may be not helpful for the Keil-Schnell type longitudinal microwave instability. This method was first applied successfully with a third harmonic cavity to increase Landau damping

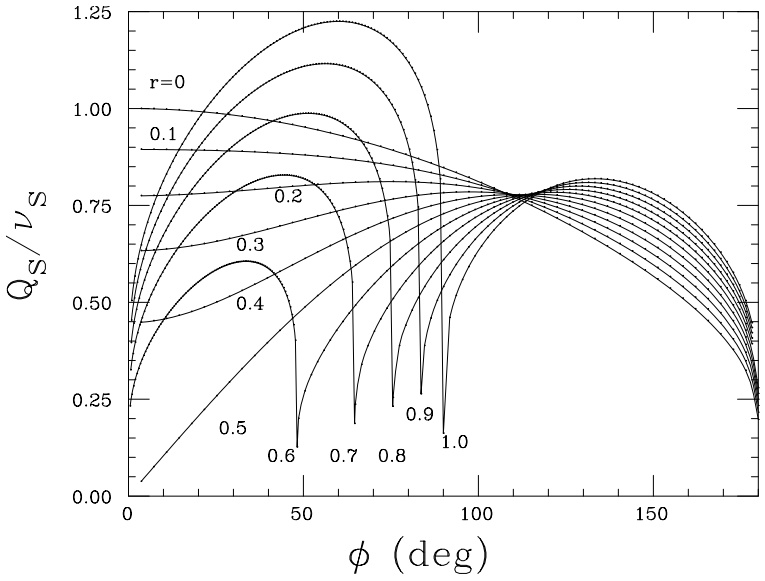

Figure 8.10: The normalized synchrotron tune of a double rf system as a function of the peak rf phase ϕ for various voltage ratio r. Here, the higher-harmonic cavity has frequency twice that of the fundamental. When $r > \frac{1}{2}$, the center of the bucket becomes an unstable fixed point and two stable fixed points emerge [5].

at the Cambridge Electron Accelerator (CEA) [6]. It was later applied at the ISR with a 6th harmonic cavity to cure mode-mixing instability [7]. Recently, a third-harmonic cavity has been reported in the SOLEIL ring in France to give a relative frequency spread of about 200%. However, since the center frequency has been dramatically decreased (not exactly to zero), the net result is a poor improvement in the stabilization. The gain in the stability threshold has been only 30% [4].

Actually, with a higher-harmonic cavity, the bunch becomes more rectangular-like in the longitudinal phase space, or particles are not so concentrated at the center of the bunch. Assuming the bunch area to be the same, the Boussard-modified Keil-Schnell threshold is proportional to the energy spread. Since the bunch becomes more flattened, the maximum energy spread which is at the center of the bunch is actually reduced, and so will be the instability threshold. However, spreading out the particles longitudinally does help to increase the bunching factor and decrease the incoherent self-field or space-charge tune shift. At the Proton Synchrotron Booster at CERN, a rf system with higher harmonics 5 to 10 has raised the beam intensity by about 25 to 30% [8]. For the Cooler Ring at the Indiana University Cyclotron Facility, a double cavity has been able to

quadruple the beam intensity [5].

8.3.2 PASSIVE LANDAU CAVITY

Higher-harmonic cavities are useful in producing a large spread in synchrotron frequency so that single-bunch mode-mixing instability and coupled-bunch instability can be damped. However, the power source to drive this higher-harmonic rf system can be rather costly. One way to overcome this is to do away with the power source and let the higher-harmonic cavity or cavities be driven by the beam-loading voltage of the circulating beam.

For a cavity with a high quality factor, the beam loading voltage is just the i_b, the current component at the cavity resonant frequency, multiplied by the impedance of the cavity. Here, for a Gaussian bunch

$$i_b = 2I_0 e^{-\frac{1}{2}(mh\omega_0\sigma_\tau)^2} \ , \tag{8.64}$$

where σ_τ is the rms bunch length and $\omega_0/(2\pi)$ is the revolution harmonic. The ratio of the resonant frequencies of the higher-harmonic cavity to the fundamental rf cavity is m and h is the fundamental rf harmonic. Thus for a short bunch, $i_b \approx 2I_0$ with I_0 being the average current of the bunch.

The higher-harmonic cavity must have suitable shunt impedance R_s and quality factor Q, and this can be accomplished by installing necessary resistor across the cavity gap. Thus, R_s and Q can be referred to as the loaded quantities of the cavity. For a particle arriving at time τ ahead of the synchronous particle, it sees the total voltage

$$V(\tau) = V_{\rm rf}\sin(\phi_s - \omega_{\rm rf}\tau) - i_b R_s \,\mathcal{R}e\left[\frac{1}{1+i2Q\delta}e^{im\omega_{\rm rf}\tau}\right] - \frac{U_s}{e} \ , \tag{8.65}$$

where $\omega_{\rm rf} = h\omega_0$ is the angular rf frequency determined by the resonator in the rf klystron that drives the fundamental rf cavity and the negative sign in front of i_b indicates that this beam loading voltage is induced by the image current and opposes the beam current. In above,

$$\delta = \frac{1}{2}\left(\frac{\omega_r}{m\omega_{\rm rf}} - \frac{m\omega_{\rm rf}}{\omega_r}\right) \approx \frac{\omega_r - m\omega_{\rm rf}}{\omega_r} \tag{8.66}$$

represents the deviation of the resonant angular frequency ω_r of the higher-harmonic cavity from the mth multiple of the rf angular frequency. Of course, this is related to

the detuning angle ψ of the higher-harmonic cavity, which we introduce in the usual way as

$$\tan\psi = 2Q\delta \ . \tag{8.67}$$

Now, Eq. (8.65) can be rewritten as

$$V(\tau) = V_{\rm rf}\sin(\phi_s - \omega_{\rm rf}\tau) - i_b R_s \cos\psi\cos(\psi - m\omega_{\rm rf}\tau) - \frac{U_s}{e} \ . \tag{8.68}$$

Again to acquire the largest spread in synchrotron frequency, we require

$$V(0) = 0\,, \quad V'(0) = 0\,, \quad V''(0) = 0\,, \tag{8.69}$$

so that the potential for small amplitudes becomes quartic,

$$U(\tau) = -\int V(\tau)d\tau = -\frac{\tau^4}{4!}V'''(0) \ . \tag{8.70}$$

Since we are having exactly the same quartic potential as in an rf system with an active Landau cavity, we expect the synchrotron frequency to be exactly the same as the expression given by Eq. (8.62) when the oscillation amplitude is small.

The set of requirements, however, are different from that of the active Landau cavity system. Here, the requirements are

$$V_{\rm rf}\sin\phi_s \ = \ i_b R_s\cos^2\psi + U_s/e \ , \tag{8.71}$$

$$V_{\rm rf}\cos\phi_s \ = \ -m\, i_b R_s\cos\psi\sin\psi \ , \tag{8.72}$$

$$V_{\rm rf}\sin\phi_s \ = \ m^2 i_b R_s\cos^2\psi \ . \tag{8.73}$$

For an electron machine which is mostly above transition, the synchronous angle ϕ_s is between $\frac{1}{2}\pi$ and π. Thus, from Eq. (8.72), we immediately obtain

$$\sin 2\psi > 0 \Longrightarrow 0 < \psi < \frac{\pi}{2} \ , \tag{8.74}$$

and from Eqs. (8.66) and (8.67), $\omega_r > m\omega_{\rm rf}$. This means that the beam in the higher-harmonic cavity is Robinson unstable [4], as is illustrated in Fig. 8.11. Of course, the fundamental rf cavity should be Robinson stable, and it will be nice if the detuning is so chosen that the beam remains stable after traversing both cavities.

The synchrotron light source electron ring at LNLS, Brazil would like to install a passive Landau cavity with $m = 3$ in order to alleviate the longitudinal coupled-bunch instabilities. The fundamental rf system has harmonic $h = 148$ or rf frequency

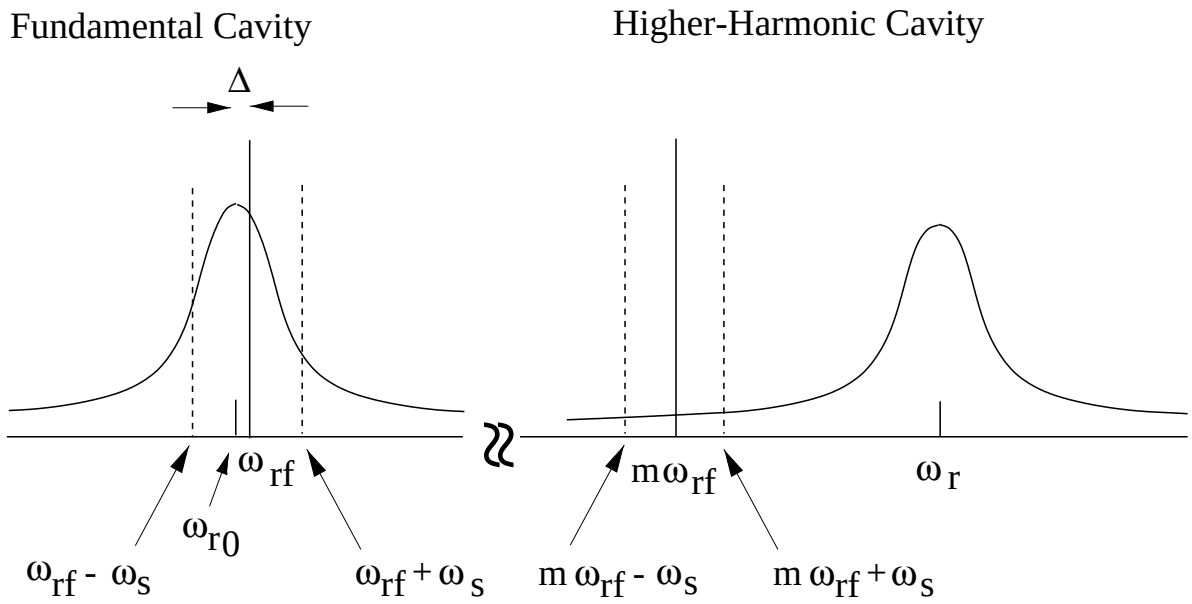

Figure 8.11: For the higher-harmonic cavity, the resonant frequency ω_r is above the mth multiple of the rf frequency. The beam will be Robinson unstable above transition. For the fundamental cavity, the resonant frequency ω_{r0} is below the rf frequency $\omega_{\rm rf} = h\omega_0$, and the beam will be Robinson stable. The detuning of the fundamental rf should be so chosen that the beam will be stable after traversing both cavities.

$f_{\rm rf} = \omega_{\rm rf}/(2\pi) = 476.0$ MHz with a tuning range of ± 10 kHz, and rf voltage $V_{\rm rf} = 350$ kV. To overcome the radiation loss, the synchronous phase is set at $\phi_{s0} = 180^\circ - 19.0^\circ$. This gives a synchrotron tune at small amplitudes $\nu_s = 6.87\times 10^{-3}$ or a synchronous frequency $f_s = 22.1$ kHz.

With the installation of the passive Landau cavity, the synchronous phase must be modified to a new ϕ_s, which is obtained by solving Eqs. (8.71) and (8.73):

$$\sin\phi_s = \left(\frac{m^2}{m^2-1}\right)\left(\frac{U_s}{eV_{\rm rf}}\right) = \frac{m^2}{m^2-1}\sin\phi_{s0}\ . \tag{8.75}$$

Thus,

$$\phi_{s0} = 180^\circ - 19.0^\circ \quad \Longrightarrow \quad \phi_s = 180^\circ - 21.49^\circ\ , \tag{8.76}$$

where $m = 3$ has been used. The detuning ψ of the higher-harmonic cavity can be

obtained from Eqs. (8.72) and (8.73), or

$$\tan\psi = -m\cot\phi_s \quad \Longrightarrow \quad \psi = 82.53^\circ \ . \tag{8.77}$$

Finally from Eq. (8.73),

$$i_b R_s = \frac{V_{\rm rf}\sin\phi_s}{m^2\cos^2\psi} \ . \tag{8.78}$$

With $i_b = 2I_0 = 0.300$ A and $V_{\rm rf} = 350$ kV, we obtain the shunt impedance of the higher-harmonic cavity to be $R_s = 2.81$ MΩ. The power taken out from the beam is

$$P = \frac{1}{2}\,\frac{i_b^2 R_s}{1+\tan^2\psi} = 2.14 \text{ kw} \ , \tag{8.79}$$

which is not large when compared with the power loss due to radiation

$$P_{\rm rad} = NU_s f_0 = I_0 V_{\rm rf}\sin\phi_{s0} = 17.09 \text{ kw} \ , \tag{8.80}$$

where N is the number of electrons in the bunch. The higher-harmonic cavity has a quality factor of $Q = 45000$ and a resonant frequency $f_r \sim 3f_{r0} = 1428$ MHz. From the detuning, it can easily found that the frequency offset is $f_r - 3f_{\rm rf} = 121$ kHz.

Now let us compute the growth rate for one bunch at the coherent frequency Ω. For one particle of time advance τ, we have from Sacherer integral equation for a short bunch [2],

$$\Omega^2 - \omega_s(\tau)^2 = \frac{i\eta e I_0}{E_0 T_0}\sum_q (q\omega_0+\Omega) Z_0^{\parallel}(q\omega_0+\Omega) \ . \tag{8.81}$$

where η is the slip factor and we have retained the dependency of the synchrotron frequency ω_s on τ because of its large spread in the presence of the higher-harmonic cavity. From Eq. (8.62), this dependency is

$$\frac{\omega_s(\tau)}{\omega_{s0}} = \frac{\pi}{2}\left(\frac{m^2-1}{6}\right)^{1/2}\frac{\omega_{\rm rf}\tau}{K(1/\sqrt{2})}\sqrt{\frac{\cos\phi_s}{\cos\phi_{s0}}}\left[\frac{1-\left(\dfrac{m^2}{m^2-1}\,\dfrac{U_s}{eV_{\rm rf}}\right)^2}{1-\left(\dfrac{U_s}{eV_{\rm rf}}\right)^2}\right]^{1/4} \ , \tag{8.82}$$

where the last factor amounts to 0.9920 and can therefore be safely abandoned. Thus, the average ω_s^2 over the whole bunch just gives the square of the rms frequency spread,

$$\langle\omega_s^2\rangle = \sigma_{\omega_s}^2 = \left[\frac{\pi\omega_{s0}}{2}\sqrt{\frac{m^2-1}{6}}\,\frac{\omega_{\rm rf}\sigma_\tau}{K(1/\sqrt{2})}\right]^2 \ . \tag{8.83}$$

The FWHM natural bunch length at $V_{\rm rf} = 350$ kV is 70.6 ps; thus $\sigma_\tau = 30.0$ ps. This gives $\sigma_{\omega_s} = 12.2$ kHz.

Since the synchrotron frequency is now a function of the offset from the stable fixed point of the rf bucket, a dispersion relation can be obtained from Eq. (8.81) by integrating over the synchrotron frequency distribution of the bunch. Here, we are interested in the growth rate without damping, which is given approximately by

$$\frac{1}{\tau} = \mathcal{I}m\,\Omega \approx \frac{\eta e I_0 \omega_{\rm rf}}{2E_0 T_0 (2\sigma_{\omega_s})} \left\{ \left[\mathcal{R}e\, Z_0^{\parallel}(\omega_{\rm rf} + 2\sigma_{\omega_s}) - \mathcal{R}e\, Z_0^{\parallel}(\omega_{\rm rf} - 2\sigma_{\omega_s}) \right] \right.$$
$$\left. + m \left[\mathcal{R}e\, Z_0^{\parallel}(m\omega_{\rm rf} + 2\sigma_{\omega_s}) - \mathcal{R}e\, Z_0^{\parallel}(m\omega_{\rm rf} - 2\sigma_{\omega_s}) \right] \right\} \ , \tag{8.84}$$

where the mean angular synchrotron frequency has been assumed to be

$$\bar{\omega}_s = 2\sigma_{\omega_s} \ . \tag{8.85}$$

This can be computed easily by substituting into the expression for $\mathcal{R}e\, Z$. However, the differences in Eq. (8.84) can also be approximated by derivatives. For the higher-harmonic cavity, both the upper and lower synchrotron side-bands lie on the same side of the higher-harmonic resonance as indicated in Fig. 8.11. Also their difference, $4\sigma_\omega/(2\pi) = 7.76$ kHz is very much less than the cavity detuning $(\omega_r - m\omega_{\rm rf})/(2\pi) = 121$ kHz. Recalling that

$$\mathcal{R}e\, Z(\omega) = R_s \cos^2\psi \ , \tag{8.86}$$

where the detuning ψ is given by Eq. (8.67), the second term can be written as a differential,

$$\mathcal{R}e\, Z_0^{\parallel}(m\omega_{\rm rf} + 2\sigma_{\omega_s}) - \mathcal{R}e\, Z_0^{\parallel}(m\omega_{\rm rf} - 2\sigma_{\omega_s}) \approx \left[R_s \cos^2\psi \sin 2\psi \, \frac{2Q}{\omega_r} \right] 4\sigma_{\omega_s} \ . \tag{8.87}$$

For the fundamental cavity, the detuning is usually $\Delta = -10$ kHz at injection and is reduced to $\Delta = -2$ kHz in storage mode when the highest electron energy is reached. Thus, the upper and lower synchrotron side-bands lie on either side of the resonance as illustrated in Fig. 8.11. Since $\Delta \ll \sigma_{\omega_s}$, we can also write the first term of Eq. (8.84) as a differential about $(2\sigma_{\omega_s})$. Thus,

$$\mathcal{R}e\, Z_0^{\parallel}(\omega_{\rm rf} + 2\sigma_{\omega_s}) - \mathcal{R}e\, Z_0^{\parallel}(\omega_{\rm rf} - 2\sigma_{\omega_s})$$
$$= \mathcal{R}e\, Z_0^{\parallel}(\omega_{r0} + \Delta + 2\sigma_{\omega_s}) - \mathcal{R}e\, Z_0^{\parallel}(\omega_{r0} - \Delta + 2\sigma_{\omega_s}) \approx \left[R_s \cos^2\psi_{\omega_s} \sin 2\psi_{\omega_s} \, \frac{2Q}{\omega_{r0}} \right] 2\Delta \ , \tag{8.88}$$

where $\omega_{r0}/(2\pi) = 476.00$ MHz is the resonance frequency of the fundamental cavity and ψ_{ω_s}, which is similar to a detuning angle, is defined as

$$\tan\psi_{\omega_s} = 2Q\,\frac{2\sigma_{\omega_s}}{\omega_{r0}}\ . \tag{8.89}$$

We arrive at

$$\frac{1}{\tau} = \frac{2\eta e I_0 Q}{E_0 T_0}\left[\frac{2\Delta}{2\sigma_{\omega_s}}\ R_s\cos^2\psi_{\omega_s}\sin 2\psi_{\omega_s}\Big|_{\text{fundamental}} + R_s\cos^2\psi\sin 2\psi\Big|_{\text{higher harmonic}}\right]\ . \tag{8.90}$$

The square bracketed factor in Eq. (8.90) becomes

$$\left[\frac{2\Delta}{2\sigma_{\omega_s}}\ R_s\cos^2\psi\sin 2\psi\Big|_{\text{fundamental}} + R_s\cos^2\psi\sin 2\psi\Big|_{\text{higher}}\right] = (-0.0059 + 0.0122)\ \text{M}\Omega\ , \tag{8.91}$$

where we have used for the fundamental cavity, the shunt impedance $R_s = 3.84$ MΩ, and quality factor $Q = 45000$. The growth rate is 1680 s^{-1} or a growth time of 0.596 ms, which is very fast. Note that the assumption of the mean synchrotron angular frequency in Eq. (8.85) is not sensitive to the higher-harmonic-cavity term in Eq. (8.84) but is rather sensitive to the fundamental-cavity term. For example, if we use $\bar{\omega}_s = 2.5\sigma_{\omega_s}$, the growth time decreases to 0.389 ms, while $\bar{\omega}_s = 1.5\sigma_{\omega_s}$ makes the system Robinson stable. With this uncertainty, it may be better to increase the detuning Δ of the fundamental.

Now let us estimate how large a Landau damping we obtain from the passive Landau cavity coming from the spread of the synchrotron frequency. Following Eq. (8.38), the stability criterion is roughly

$$\frac{1}{\tau} \lesssim \frac{\omega_s(\sqrt{6}\sigma_\tau)}{4}\ , \tag{8.92}$$

where the synchrotron angular frequency spread is given by Eq. (8.62). The spread in synchrotron angular frequency has been found to be $\omega_s(\sqrt{6}\sigma_\tau) = 39.6$ kHz. In other words, the higher-harmonic cavity is able to damp an instability that has a growth time longer than 0.101 ms, an improvement of 57 folds better than when the higher-harmonic cavity is absent. Thus, theoretically, this Landau damping is large enough to alleviate the Robinson antidamping of higher-harmonic cavity.

We notice that the required shunt impedance of the passive Landau cavity $R_s = 2.81$ MΩ is large, although it is still smaller than the shunt impedance of 3.84 MΩ of the fundamental cavity. It is easy to understand why such large impedance is required. The synchronous angle for a storage ring without the Landau cavity is usually just not too

much from 180°, here $\phi_{s0} = 180° - 19.0°$, because of the compensation of a small amount of radiation loss. The rf gap voltage phasor is therefore almost perpendicular to the beam current phasor. In order that the beam-loading voltage contributes significantly to the rf voltage, the detuning angle of the passive higher-harmonic cavity must therefore be large also, here $\psi = 82.53°$. In fact, without radiation loss to compensate, the beam-loading voltage phasor would have been exactly perpendicular to the beam current phasor. Since $\cos\psi = 0.130$ is small, the shunt impedance of the higher-harmonic cavity must therefore be large. In some sense, the employment of the higher-harmonic cavity is not efficient at all, because we are using only the tail of a large resonance impedance, as is depicted in Fig. 8.11. This is not a waste at all, however, because we can do away with the generating source for this cavity. Also, the large detuning angle implies not much power will be taken out from the beam as it loads the cavity, only 2.14 kw here. On the other hand, the detuning of the fundamental cavity need not be too large. This is because the rf gap voltage is supplied mostly by the generator voltage and only partially by the beam loading in the cavity.

The most important question here is how do we generate a large shunt impedance for the higher-harmonic cavity. Usually it is easy to lower the shunt impedance by adding a resistor across the cavity gap. Some other means will be required to raise the shunt impedance, in case it is not large enough. One way is to coat the interior of the higher-harmonic cavity with a layer of medium that has a higher conductivity. However, it is hard to think of any medium that has a conductivity very much higher than the copper surface of the cavity. For example, the conductivity of silver is only slightly higher. Another way to increase the conductivity significantly is the reduction of temperature to the cryogenic region. Notice that R_s/Q is a geometric property of the cavity. Raising R_s will raise Q also. However, a higher quality factor is of no concern here, because the requirements in Eqs. (8.71), (8.72), and (8.73) depend on the detuning ψ only and are independent of Q. With the same detuning ψ, a higher Q just implies a smaller frequency offset between the resonant angular frequency ω_r of the higher-harmonic cavity and the mth multiple of the rf angular frequency.

Another way to achieve a lower shunt impedance requirement is to reduce the rf voltage. We can rewrite Eq. (8.78) as

$$i_b R_s = \frac{U_s}{e}\left[\left(\frac{m^2-1}{m^2}\right)^2\left(\frac{eV_{\rm rf}}{U_s}\right)^2 - \frac{m^2-1}{m^2}\right] , \tag{8.93}$$

after eliminating ϕ_s and ψ with the aid of Eqs. (8.75) and (8.77). Thus, for a given beam

current, lowering $V_{\rm rf}$ will result in a smaller shunt impedance. Notice that the right side is quadratic in $V_{\rm rf}$, a higher $V_{\rm rf}$ will increase the required shunt impedance by very much. For example, with the same radiation loss, increasing $V_{\rm rf}$ from 350 kV to 500 kV will increase the required shunt impedance of the higher-order cavity from 2.61 to 6.12 MΩ. However, lowering $V_{\rm rf}$ by too much is usually not favored because the electron bunches will become too long.

There is a big difference between an active Landau cavity and a passive Landau cavity. In an active Landau cavity, the criteria of Eq. (8.60) are independent of the beam intensity. On the other hand, the criteria for the operation of a passive cavity, Eqs. (8.71), (8.72), and (8.73), depend on the bunch intensity. What will happen when the bunch intensity changes significantly? Let us recall how we arrive at the solution of the 3 equations of the passive two-rf system. The new synchronous phase ϕ_s, as given by Eq. (8.75), is determined solely by the ratio of the radiation loss U_s to the rf voltage $V_{\rm rf}$. while the detuning ψ is just given by $-m\cot\phi_s$. The only parameter that depends on the beam current is the shunt impedance R_s. Therefore, if the bunch intensity is different, one can adjust the rf voltage so that Eq. (8.93) remains satisfied with the new current but with the preset R_s. With the new rf voltage, the synchronous phase ϕ_s has to be adjusted so that Eq. (8.75) remains satisfied. It will be best if the detuning ψ can be also adjusted according to Eq. (8.77). Unfortunately, this is not possible, because a change in ψ is equivalent to a change in the resonant frequency of the cavity. In other words, unless the intensity of the bunch is carefully controlled to meet the designed requirement, most of the time, a synchrotron frequency given by Eq. (8.62) cannot be realized. As is shown in Fig. 8.10 for a $m = 2$ double rf system, when the rf voltage ratio deviates from $r = 1/m = 0.5$ by 20% to 0.4, the spread in synchrotron frequency for a small bunch decreases tremendously to almost the same tiny value as in the single rf system. For this reason, in order for a passive Landau cavity to work, the bunch intensity must be kept relatively constant from cycle to cycle, with a difference not exceeding a couple of percents.

8.3.3 RF VOLTAGE MODULATION

The modulation of the rf system will create nonlinear parametric resonances, which redistribute particles in the longitudinal phase plane. The formation of islands within an rf bucket reduces the density in the bunch core. As a result, beam dynamics properties related to the bunch density, such as beam life time, beam collective instabilities, etc, can be improved.

Here we try to modulate the rf voltage with a frequency $\nu_m\omega_0/(2\pi)$ and amplitude ϵ, so that the energy equation becomes [9]

$$\frac{d\Delta E}{dn} = eV_{\rm rf}[1+\epsilon\sin(2\pi\nu_m n+\xi)][\sin(\phi_s - h\omega_0\tau) - \sin\phi_s] - [U(\delta) - U_s] \ , \qquad (8.94)$$

where ξ is a randomly chosen phase and ν_m the modulating tune. This modulation will introduce resonant island structure in the longitudinal phase plane. There are two critical tunes:

$$\begin{cases} \nu_1 = 2\nu_s + \frac{1}{2}\epsilon\nu_s \ , \\ \nu_2 = 2\nu_s - \frac{1}{2}\epsilon\nu_s \ . \end{cases} \qquad (8.95)$$

If we start the modulation by gradually increasing the modulating tune ν_m towards ν_2 from below, two islands appear inside the bucket from both sides, as shown in the second plot of Fig. 8.12. The phase space showing the islands is depicted in Fig. 8.13. As ν_m is increased, these two islands come closer and closer to the center of the bucket and the particles in the bunch core gradually spill into these two islands, forming 3 beamlets. When ν_m reaches ν_2, the central core disappears and all the particles are shared by the two beamlets in the two islands. Further increase of ν_m above ν_2 moves the two beamlets closer together. When ν_m equals ν_1, the two beamlets merge into one. Under all these situations, the two outer islands rotate around the center of the rf bucket with frequency equal to one half the modulation frequency.

Rf voltage modulation has been introduced into the light source SRRC at Taiwan to cope with longitudinal coupled-bunch instability [10]. A modulation frequency slightly below twice the synchrotron frequency with 10% voltage modulation was applied to the rf system. The beam spectrum measured from the BPM sum from a HP4396A network analyzer before and after the modulation is shown in Fig. 8.14. It is evident that the intensity of the beam spectrum has been largely reduced after the application of the modulation. The sidebands around the harmonics of 587.106 Hz and 911.888 MHz are magnified in Fig. 8.15. We see that the synchrotron sidebands have been suppressed by very much. The multibunch beam motion under rf voltage modulation was also recorded by streak camera, which did not reveal any coupled motion of the bunches.

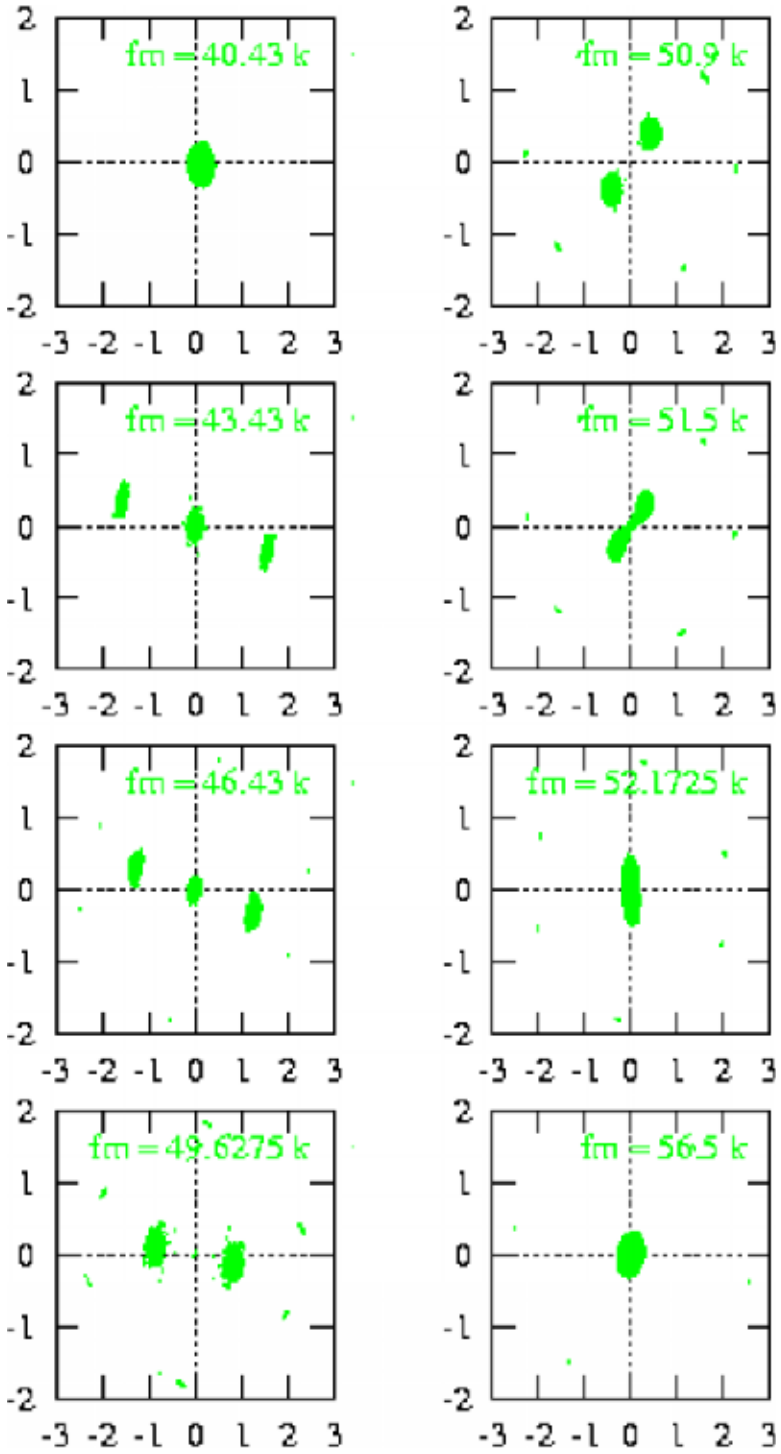

Figure 8.12: (Color) Simulation results of rf voltage modulation. The modulation frequency is increased from top to bottom and left to right. The modulation amplitude is 10% of the cavity voltage. The 4th plot is right at critical frequency $\nu_2 f_0 = 49.6275$ kHz and the 7th plot right at critical frequency $\nu_1 f_0 = 52.1725$ kHz.

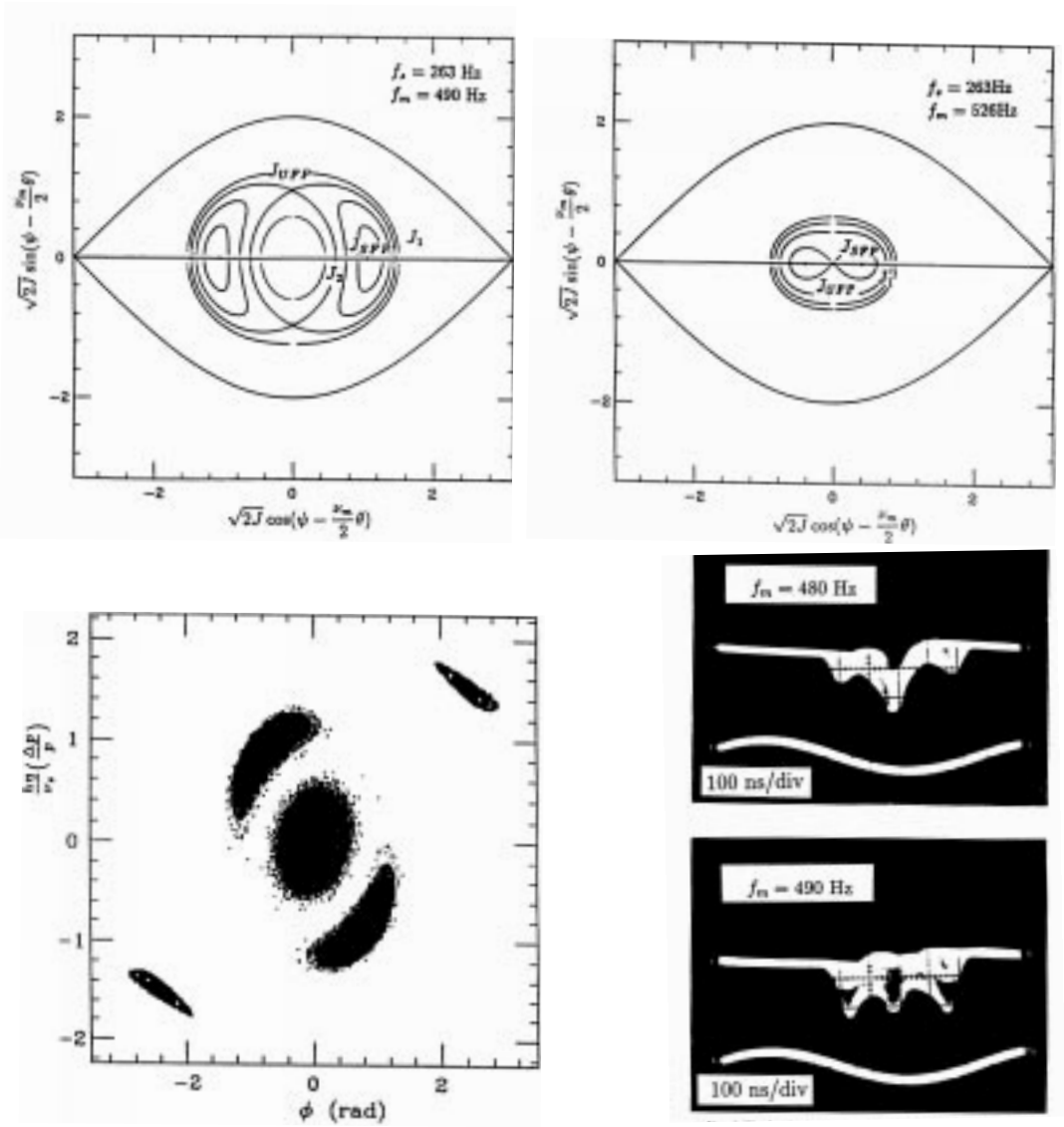

Figure 8.13: Top figures show separatrices and tori of the time-independent Hamiltonian with voltage modulation in multiparticle simulation for an experiment at IUCF. The modulation tune is below ν_2 with the formation of 3 islands on the left, while the modulation tune is above ν_2 with the formation of 2 islands on the right. The lower-left plot shows the final beam distribution when there are 3 islands, a damping rate of 2.5 s^{-1} has been assumed. The lower-right plot shows the longitudinal beam distribution from a BPM sum signal accumulated over many synchrotron periods. Note that the outer two beamlets rotate around the center beamlet at frequency equal to one-half the modulation frequency.

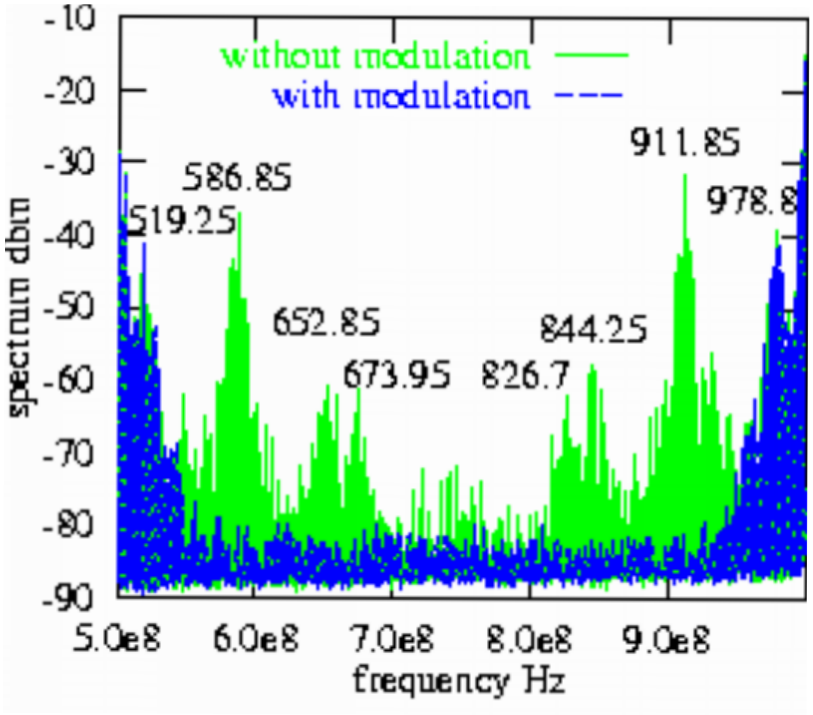

Figure 8.14: (Color) Beam spectrum from BPM sum signal before and after applying rf voltage modulation. The modulation frequency was 50.155 kHz and the voltage modulation was 10%. The frequency span of the spectrum is 500 MHz.

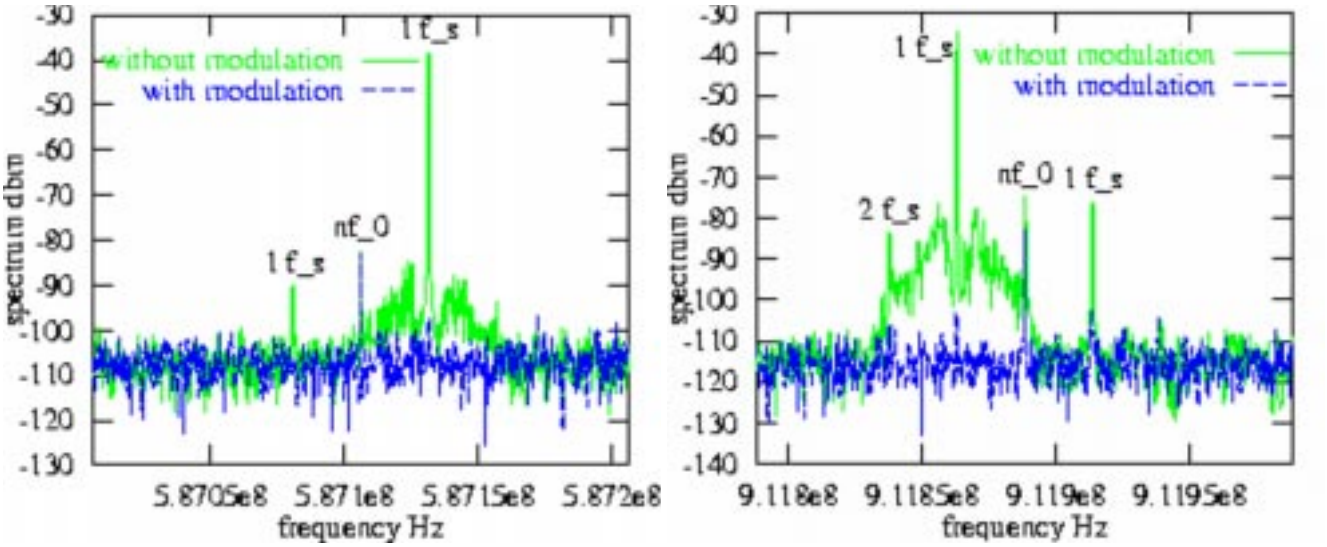

Figure 8.15: (Color) Beam spectrum zoom in from Fig. 8.14. The revolution harmonic frequency of the left is 587.106 MHz and the right is 911.888 MHz. The frequency span of the spectrum is 200 kHz.

8.4 EXERCISES

8.1. Above/below transition, with the angular resonant frequency ω_r offset by $\Delta\omega = \pm(\omega_r - h\omega_0)$ where $\omega_{\rm rf} = h\omega_0$ is the angular rf frequency, the bunch suffers Robinson's instability.

(1) Assuming that $\omega_s \ll |\Delta\omega| \ll \omega_{\rm rf}$ and using the expression for resonant impedance in Eq. (1.34), show that the Robinson growth rate in Eq. (8.34) can be written as

$$\frac{1}{\tau} = \frac{2e^2 N R_s}{E_0 T_0^2} \cos^2\psi \sin 2\psi \ , \tag{8.96}$$

where N is the number of particles in the bunch, E_0 is the synchronous energy E_0, $T_0 = 2\pi/\omega_0$ is the revolution period, and the detuning angle ψ is defined as

$$\tan\psi = 2Q\frac{\omega_r - \omega_{\rm rf}}{2\omega_r}$$

for the resonant impedance with shunt impedance R_s, resonant frequency $\omega_r/(2\pi)$, and quality factor Q.

(2) Assuming further that $|\Delta\omega|$ is much less than the resonator width $\omega_r/(2Q)$ which, in turn, is much less than ω_0, show that the Robinson growth rate can be written as

$$\frac{1}{\tau} = \frac{4e^2 N R_s Q^2 \eta \Delta\omega}{\pi\beta^2 E_0 h T_0} \ . \tag{8.97}$$

(c) Robinson's instability is usually more pronounced in electron than proton machines because high shunt impedance and quality factor are often required in the rf system. Take for example a ring of circumference 180 m with slip factor $|\eta| = 0.03$. To store a typical bunch with 1×10^{11} electrons at $E_0 = 1$ GeV, one may need a rf system with $h = 240$, $R_s = 1.0$ MΩ, and $Q = 2000$. On the other hand, to store a bunch of 1×10^{11} protons at kinetic energy $E_0 = 1$ GeV in the same ring, one may need a rf system with $h = 4$, $R_s = 0.12$ MΩ, and $Q = 45$. Compare the Robinson growth rates for the two situations when the resonant frequencies are offset in the wrong directions by $|\Delta\omega| = \omega_s$. Assume the synchrotron tune to be 0.01 in both cases.

8.2. Using the definition of the form factor in Eq. (8.53), compute numerically the form factor when the unperturbed distribution is bi-Gaussian. The half bunch length can be taken as $\hat{\tau} = \sqrt{6}\sigma_\tau$, where σ_τ is the rms bunch length.

8.3. Consider a single sinusoidal rf system operating at synchronous angle $\phi_s = 0$.
(1) Show that the synchrotron frequency of a particle at rf phase ϕ is given by

$$\frac{f_s(\phi)}{f_{s0}} = \frac{\pi}{2K(t)} \,, \tag{8.98}$$

where $t = \sin\phi/2$, f_{s0} is the synchrotron frequency at zero amplitude, and $K(t)$ is the complete elliptic integral of the first kind defined in Eq. (8.63).
(2) Show that Eq. (8.98) is consistent with Eq. (8.37) at small amplitude.

8.4. Solve the set of equations in Eq. (8.60) to obtain the fundamental rf phase ϕ_s, the higher-harmonic rf phase ϕ_m and the voltage ratio r in terms of the harmonic ratio m and $U_s/eV_{\rm rf}$.
Answer:

$$\sin\phi_s = \frac{m^2}{m^2-1}\frac{U_s}{eV_{\rm rf}} \,, \quad \tan\phi_m = \frac{\dfrac{m}{m^2-1}\dfrac{U_s}{eV_{\rm rf}}}{\sqrt{1-\left(\dfrac{m^2}{m^2-1}\dfrac{U_s}{eV_{\rm rf}}\right)^2}} \,, \quad r = \sqrt{\frac{1}{m^2} - \frac{1}{m^2-1}\frac{U_s^2}{(eV_{\rm rf})^2}} \,.$$

8.5. Derive the small amplitude synchrotron frequency as given by Eq. (8.62).

Bibliography

[1] P.B. Robinson, *Stability of Beam in Radiofrequency System*, Cambridge Electron Accel. Report CEAL-1010, 1964.

[2] F.J. Sacherer, *A Longitudinal Stability Criterion for Bunched Beams*, CERN report CERN/MPS/BR 73-1, 1973; IEEE Trans. Nuclear Sci. **NS 20**, 3, 825 (1973).

[3] A. Hofmann and S. Myers, *Beam Dynamics in a Double RF System*, Proc. 11th Int. Conf. High Energy Accel., Geneva, 1980.

[4] A. Mosnier, *Cures of Coupled Bunch Instabilities*, PAC'99, Paper FRBR2.

[5] S.Y. Lee *et al*, Phys. Rev. **E49**, 5717 (1994); J.Y. Liu *et al*, Phys. Rev. **E50**, R3349 (1994): J.Y. Liu *et al*, Part. Accel. **49**, 221-251 (1995).

[6] R. Averill *et al.*, Proceedings of 8th International Conference on High Energy Accelerators, CERN (1971) p. 301.

[7] P. Bramham *et al.*, Proceedings of 9th International Conference on High Energy Accelerators, CERN (1974); P. Bramham *et al.*, IEEE Trans. Nucl. Sci. **NS-24**, 1490 (1977).

[8] J.M. Baillod *et al.*, IEEE Trans. Nucl. Sci. **NS-30**, 3499 (1983); G. Galato *et al.*, Proceedings of the IEEE Particle Accel. Conference, 1987, p. 1298.

[9] D. Li, M. Ball, B. Brabson, J. Budnick, D.D. Caussyn, A.W. Chao, V. Derenchuk, S. Dutt, G. East, M. Ellison, D. Friesel, B. Hamilton, H. Huang, W.P. Jones, S.Y. Lee, J.Y. Liu, M.G. Minty, K.Y. Ng, X. Pei, A. Riabko, T. Sloan, M. Syphers, Y. Wang, Y. Yan, and P.L. Zhang, '*Effects of Rf Voltage Modulation on Particle Motion*, Nucl. Inst. Meth. **A364**, 205 (1995).

[10] M.H. Wang, Peace Chang, P.J. Chou, K.T. Hsu, C.C. Kuo, J.C. Lee, and W.K. Lau, *Experiment of RF Voltage Modulation at at SRRC*, PAC'99, Paper THA106.